Frontiers in Heat and Mass Transfer (FHMT), 16, 23 (2021)
DOI: 10.5098/hmt.16.23

Global Digital Central
ISSN: 2151-8629

Frontiers in Heat and Mass Transfer

Available at www.ThermalFluidsCentral.org

NUMERICAL ANALYSIS OF PASSIVE TWO PHASE FLUID FLOW IN A CLOSED LOOP PULSATING HEAT PIPE

Roshan Devidas Bhagat[a,*] Samir J. Deshmukh[b],

[a] Ph.D. Scholar, Prof. Ram Meghe Institute of Technology And Research, Badnera-Amravati, Maharashtra, 444701, India
[b] Associate Professor, Prof. Ram Meghe Institute of Technology And Research, Badnera-Amravati, Maharashtra, 444701, India

ABSTRACT

Numerical analysis of passive two phase fluid flow in a 3D Closed Loop Pulsating Heat Pipe (CLPHP) with turns in evaporator and condenser section is carried out. Water is used as working fluid. The volume of fluid model (VOF) is used to simulate passive two-phase fluid flow in a Closed Loop Pulsating Heat Pipe. Filling ratio (FR) of is kept in the range of 60 to 70%. The evaporator temperature is set in the range of 353 K. The condenser temperature is set in the range of 298 K. The contours of volume fraction water, wall temperature and contours of mass flow rate is studied. Analysis of fluid flow is done with various geometrical parameter for 3D Closed Loop Pulsating Heat Pipe. Alternative liquid and vapor slug formation are observed and evaporation and condensation process are visualized in the analysis.

Keywords: *Pulsating heat pipe, electronics cooling, numerical analysis*

1. INTRODUCTION

The heat pipe is capable of transferring large quantities of heat with minimum temperature drop. With the size of electronics devices shrinking day by day there need to implement effective cooling technique which will cool the electronics devices without compromising on the performance, to achieve this goal heat pipe technology looks promising. In heat pipe liquid and vapor slug/bubble transport is caused by the thermally induced pressure pulsations inside the device and no external mechanical power is required. The type of working fluid and the operating pressure inside the pulsating heat pipe depends on the operating temperature of the heat pipe. The region between evaporator and condenser is adiabatic. The heat is transfer from evaporator to condenser by the means of pulsating action of vapor and liquid slug.

The development of CFD model provide deeper understanding of the principles of thermodynamics, fluid dynamics and heat transfer within a pipe, allowing the performance of heat pipe to be enhanced for many different applications. Furthermore, modelling the complicated two-phase flow of boiling and condensation can be used for validating the experimental results. The boiling and condensation processes especially the boiling process does not depend on the actual shape of surface. The CFD model can reduce the experimental work necessary to predict the performance of system, which can then be optimised. The performance of final optimised model can be verified with the experimental results, which substantially reduces the cost.

Analysis is done to test performance of closed loop pulsating heat pipe with different working fluid and geometries to cool the temperature sensitive electronic equipment like CPU of laptop, graphics card, cooling of these devices is important to improve the performance of system, these devices generate heat during the high-end task. One of the objectives is to validate the experimental results with CFD tools and to understand the behaviour of fluid flow in narrow channels.

Khandekar and Groll (2003) conducted experiments on a PHP made of copper capillary tube of 2 mm inner diameter for three different working fluids viz. water, ethanol and R-123. The PHP was tested in vertical (bottom heat mode) as well as horizontal orientation and indicated that, a 100% filled PHP (not working in the pulsating mode but instead as a single-phase buoyancy-induced thermosyphon) is thermally better performing than a partially filled pulsating mode device under certain operating conditions.

Khandekar and Groll (2004) studied that, complete stop-over is within the loop happens a lot of times for filling magnitude relation < 50% as well as low heat input power. Stop-over development has additionally been determined for higher filling ratios. The 'self-sustained' periodic character is then lost; such a behaviour has never been according for multi-turn PHPs due to alternating periods during which bubble plugs are moving rapidly (activity phase) and 'stopping' (static phase).

Dadong and Cui (2010) indicated that the thermal resistance decreases with the rise of the heating power at an equivalent filling magnitude relation. For the pure operating fluid PHPs, the thermal resistance is decreases within the sequence of water, ethanol, methanol and acetone. Narasimha et al. (2012) studied that, at atmospheric condition; the saturation temperature is higher compared to evacuated situation. Thus, more liquid phase exists in the tube with a consequent increase in the heat transfer.

Charoensawan et al. (2003) indicated that in vertical orientation for the 2.0 mm devices, water filled devices showed higher performance as compared to R-123 and ethanol. Whereas in 1.0 mm devices, R-123 and ethanol filled devices showed comparable performance but water showing very poor results.

Bhagat and Watt, (2015) observed that the Acetone as working fluid has higher value of bond number and lesser thermal resistance whereas Methanol has higher thermal resistance and lower value of bond number. So, the working fluid with higher value of bond number gives higher

* *Corresponding author. Email: roshan.bhagat25@gmail.com*

DOI: 10.5098/hmt.16.23 ISSN: 2151-8629

thermal performance than the working fluid with lower value of bond number.

With the development of semiconductor technology, various electronic equipment has entered people's lives extensively, and the trend of miniaturization and integration greatly increases the power consumption and heat generation per unit area of these electronic equipment. So, it is urgent to strengthen the research and applications of heat transfer devices of high thermal conductivity. Fairley and Patel studied that in order to meet the work and production requirements of higher heat load, smaller design space and lower cost, the development of passive cooling system with higher performance has become a focus of research. Qu and Zhao found that as a new heat transfer device, the PHP has a series of advantages such as high heat transfer efficiency, good adaptability, simple structure and low cost. So, since it was invented in the 1990s. Kearney state that the PHP has been paid close attention by researchers due to its unique working principle and excellent heat transfer efficiency. It has been applied in a variety of fields, such as heat dissipation of electronic equipment, heat collection of solar energy, recovery of waste heat, thermal management of power units.

During the start-up period the working fluid oscillate with large amplitude, after this period continuous circulation can occurs in the working fluid occurs. The direction of circulation for working fluid is consistent once circulation is obtained but the direction of circulation can be different for same experimental run.

Working fluid is vital issue that considerably influence the thermal performance of CLPHP, since operating fluid acts as heat transferring medium between source and sink. Thermal performance of the heat pipe considerably depends on thermo dynamical properties of operating fluid. The thermo dynamical properties involving two-part flow heat transfer encompass heat energy, heat capability, viscosity, physical phenomenon etc. the choice of the operating fluid employed in PHPs is depends on many variables. The approximate temperature ranges the system are going to be exposed to be most crucial in determining the right operating fluid. Exploitation to associated degree approximate temperature variation of $-50^0C\ \ 150^0C$, suggests several potential operating fluids square measure doable choice for pulsating heat pipe.

The objective of research work is to do the numerical analysis of 3D Closed loop pulsating heat pipe. Numerical analysis is done on Various geometrical parameter having one or more turns, flat evaporator and condenser section, evaporator section with coil arrangement to visualize the complex phenomenon of evaporation and condensation.

2. Boundary Conditions

Working fluids is tested with different combination of pulsating heat pipe. More attention is given on developing 3D model with the help of CFD tools that includes the complex physical phenomenon of the heat transfer, the process of evaporation and condensation. The fluid flow behavior is observed with different sets of parameters. The use of CFD model can reduce the experimental work necessary to predict the performance of system, which can then be optimized. The performance of final optimized model can be verified with the experimental results, which substantially reduces the cost of fabrication.

2.1 Physical Characteristics and Assumption

The pulsating heat pipe used in the analysis here has inner diameter of 2mm. Various geometries with single turn, flat, multiple turns and evaporator coils. The filling ratio is taken in the range of 60 to 70%. Three phases are utilized liquid, vapor and air. Volume of fluid model is most suitable as it tracks the interphase of phases. The three Eulerian phases are air, water vapor and water liquid, even though there is a vacuum inside the pipe, which is defined later, air is still defined as one of the phases. The reason for including a phase with air is that if only water liquid and vapor are defined, the calculation starts as if there is already water vapor inside the pipe. The k-epsilon model is selected, with enhance wall treatment, thermal effect and curvature correction.

2.2 Governing Equations

The flow inside the pulsating heat pipe is having liquid and vapor slug transformation. As the phase change takes place at the saturation temperature, the conservation of mas equation needs to be taken into consideration.

$$\frac{\partial(\alpha_v\rho_v)}{\partial t}+\nabla.(\alpha_v\rho_v v_v)=\dot{m}_{lv}-\dot{m}_{vl} \tag{1}$$

The momentum equation is solved throughout the domain Eq. (2) which is reliant on volume fractions of all the phases.

$$\frac{\partial}{\partial t}(\rho\vec{v})+\nabla.(\rho\vec{v}\vec{v})=-\nabla P+\nabla.[\mu(\nabla\vec{v}+\nabla\vec{v}T)]+\rho\vec{g}+\vec{Fvol} \tag{2}$$

The energy equation shared among the phases is shown in Eq. (3). Here, Sh is energy source caused by phase change.

$$\frac{\partial}{\partial t}(\rho E)+\nabla.(\vec{v}(\rho E+P))=\nabla.(K.\nabla T+(\bar{\bar{\tau}}.\vec{v}))+Sh \tag{3}$$

Table 1 Defining the phase

Primary Phase	Vapor
Secondary Phase	Liquid
Secondary Phase	Air

2.3 Cell Zone Condition

In this section the vacuum inside the pipe is introduced. Clicking on “Cell Zone Conditions” and then on “Operating Conditions” set the “Operating Pressure” as 4000 (this is the saturation pressure of the water at a saturation temperature of 29 °C. Boundary conditions are applied in the evaporator section and temperature specified as 353 K. The condenser temperature is kept at as 298 K. As capillary action has to takes place due to smaller diameter of tube contact angle of working fluid need to be specified at all wall geometry. The contact angle is specified as 20^0.

2.4 Initializing Simulation and Patch

After configuring the other two boundary conditions i.e., evaporator and condenser the last step before starting the simulation is initializing it and attribute initial positions for the liquid and air for the beginning of the simulation. After the initialization the zones patching is done where the geometry is patch with water as working fluid. Steam portion here is considered at 0 at initial stage.

2.5 Simulation Run

The issue with simulation of multiphase flows is that the time step needs to be sufficiently small to capture the movement of the particles, and at the same time it needs to be big enough to reduce the computational time.

Table 2 Issue with different time step

Time Step	Issue
0.1	Diverge very fast
0.01	Diverges
0.001	Diverges after some time
0.0005	Takes long time but never diverge

3 Geometry & Mesh Development

3.1 Single Turn Flat Closed Loop Pulsating Heat Pipe

The 3D geometry of single turn flat closed loop pulsating heat pipe was generated with the help of Ansys Design Modeler. Default Meshing is generated with the meshing tool used in Ansys.

Table 3 Mesh information single turn flat CLPHP

Domain	Nodes	Element
Air	29826	26388
Water	33327	28920
All Domain	63153	55308

Frontiers in Heat and Mass Transfer (FHMT), 16, 23 (2021)
DOI: 10.5098/hmt.16.23 Global Digital Central
ISSN: 2151-8629

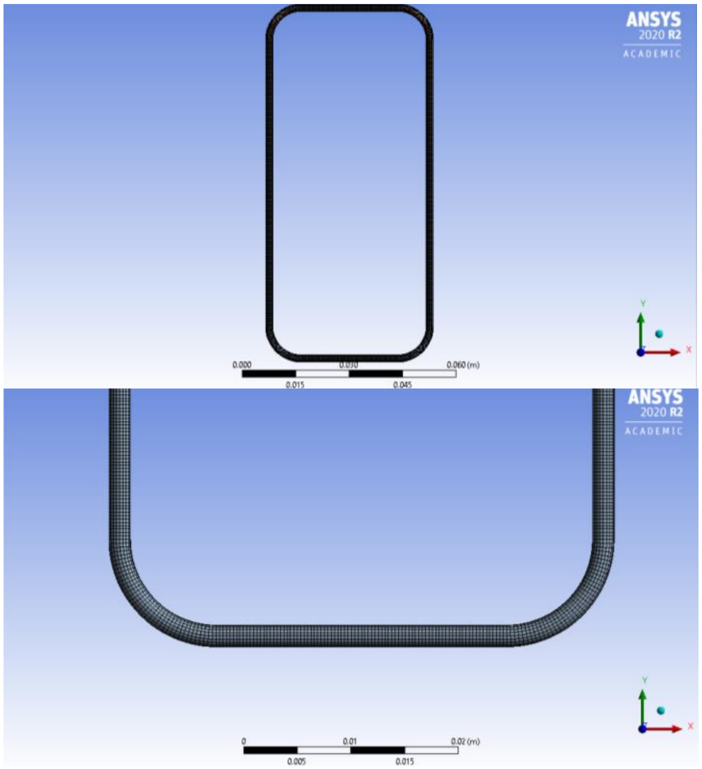

Fig. 1 Mesh generation for flat single turn CLPHP

3.2 Single Turn Closed Loop Pulsating Heat Pipe

The 3D geometry of single turn CLPHP is generated with the help of Ansys Design Modeler.

Table 4 Geometry and mesh information for single turn CLPHP

Domain	Nodes	Element
Air	30954	26867
Water	64800	58239
All Domain	95754	85106

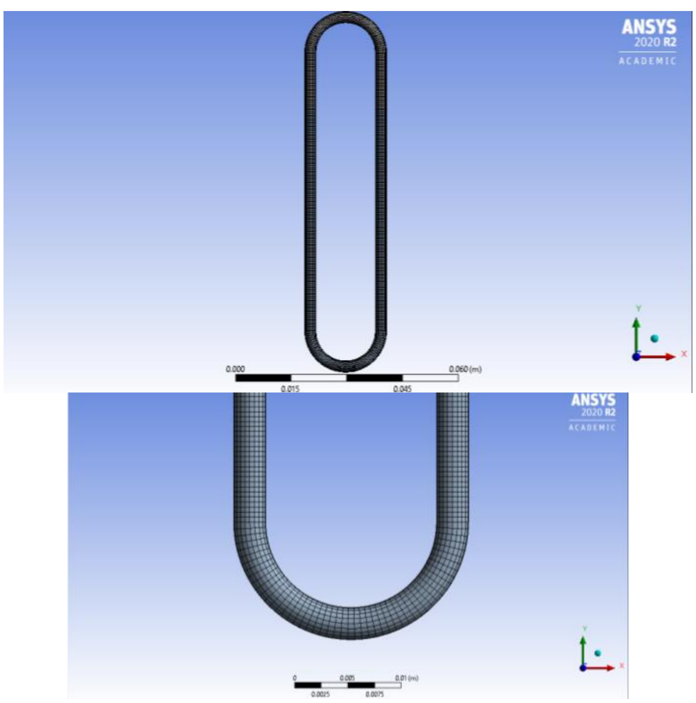

Fig. 2 Mesh generation for single turn CLPHP

Default Mesh is generated with the help of meshing tool available in Ansys. The reason for default mesh is to reduce the computational time during the process of iteration.

3.3 Two Turn Closed Loop Pulsating Heat Pipe

The 3D geometry of two turn closed loop pulsating heat pipe is generated with the help of Ansys Design Modeler. Default Meshing is done to reduce the computational time during the process of iteration. This heat pipe has two small turn in evaporator section and one large and one small turn in condenser section. The excess area of tube in condenser is to avoid dry out condition.

The geometry has inner diameter of 2mm, smaller diameter is selected to have capillary action inside the pipe.

Table 5 Geometry and mesh information for two turn CLPHP

Domain	Nodes	Element
Air	56486	50358
Water	76653	69158
All Domain	133139	119516

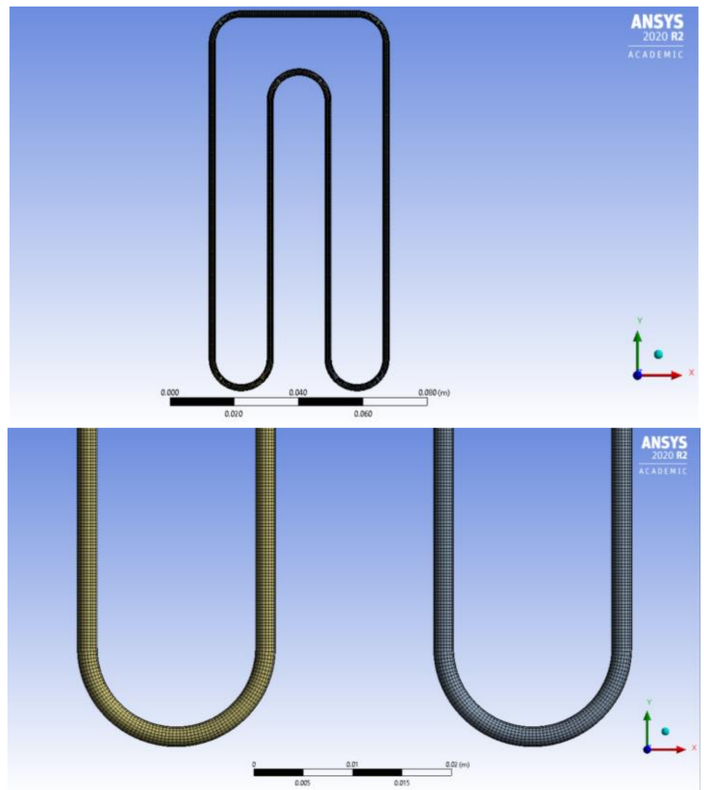

Fig. 3 Mesh generation for two turn CLPHP

3.4 Three Turn Closed Loop Pulsating Heat Pipe

The 3D geometry of three turn closed loop pulsating heat pipe is generated with the help of Ansys Design Modeler. Default Mesh is generated with the meshing tool used in Ansys. The evaporator section has three small turn and the condenser section has two small and one large turn.

The geometry has inner diameter of 2mm, smaller diameter is selected to have capillary action inside the pipe.

Table 6 Geometry and mesh information for three turn CLPHP

Domain	Nodes	Element
Air	90893	79192
Water	147600	129035
All Domain	238493	208227

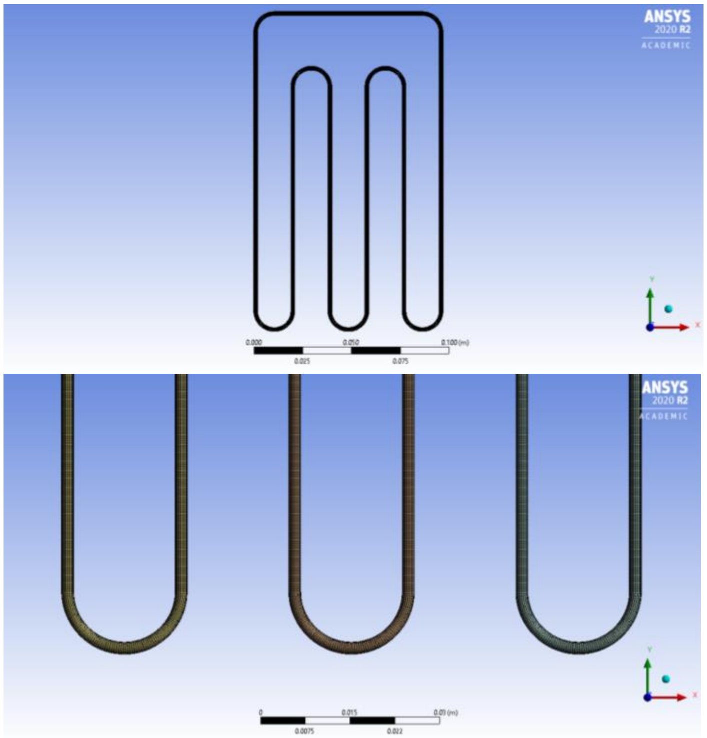

Fig. 4 Mesh generation for three turn CLPHP

3.5 Six Turn Closed Loop Pulsating Heat Pipe

The 3D geometry is created with inner diameter of 2mm.

Table 7 Geometry and mesh information for Six turn CLPHP

Domain	Nodes	Element
Air	109289	94853
Water	115005	100584
All Domain	224294	195437

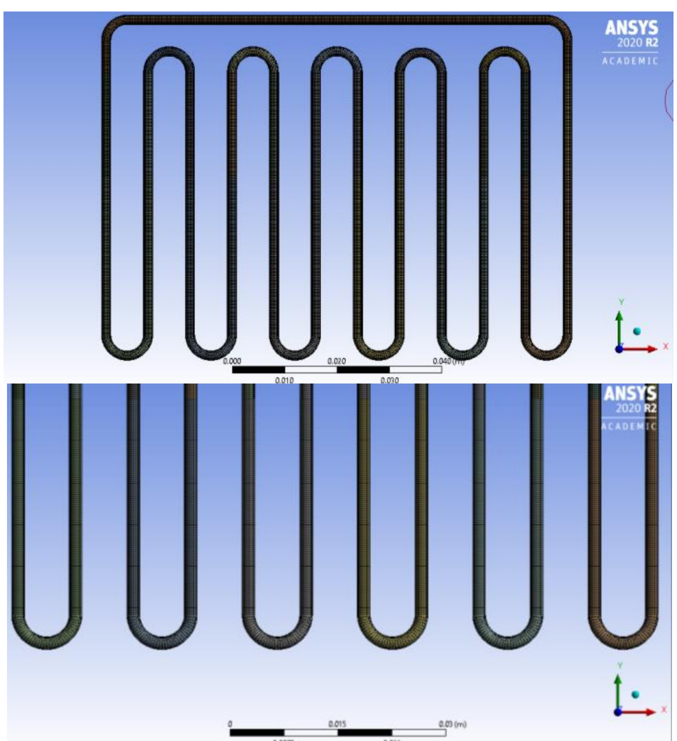

Fig. 5 Mesh generation for six turn CLPHP

The geometry of heat pipe has six small turns in evaporator section and five small and one large turn in condenser section. Surface area of copper tube in condenser section is ensure to have higher value than the evaporator section to avoid the dry out of working fluid.

3.6 Evaporator Coil Closed Loop Pulsating Heat Pipe

The 3D geometry with inner diameter of 2mm generated in Ansys Design Modeler. Sweep operation is used to prepare the turns in evaporator section. Default meshing is done to reduce computational time required. The geometry is sliced in the evaporator and condenser section, geometry slice is useful to define the heater and condenser section. Specification of heater and condenser section is required to apply the boundary condition in setup.

Table 8 Geometry and mesh information for evaporator coil CLPHP

Domain	Nodes	Element
Air	15676	13520
Water	41871	34440
All Domain	57546	47960

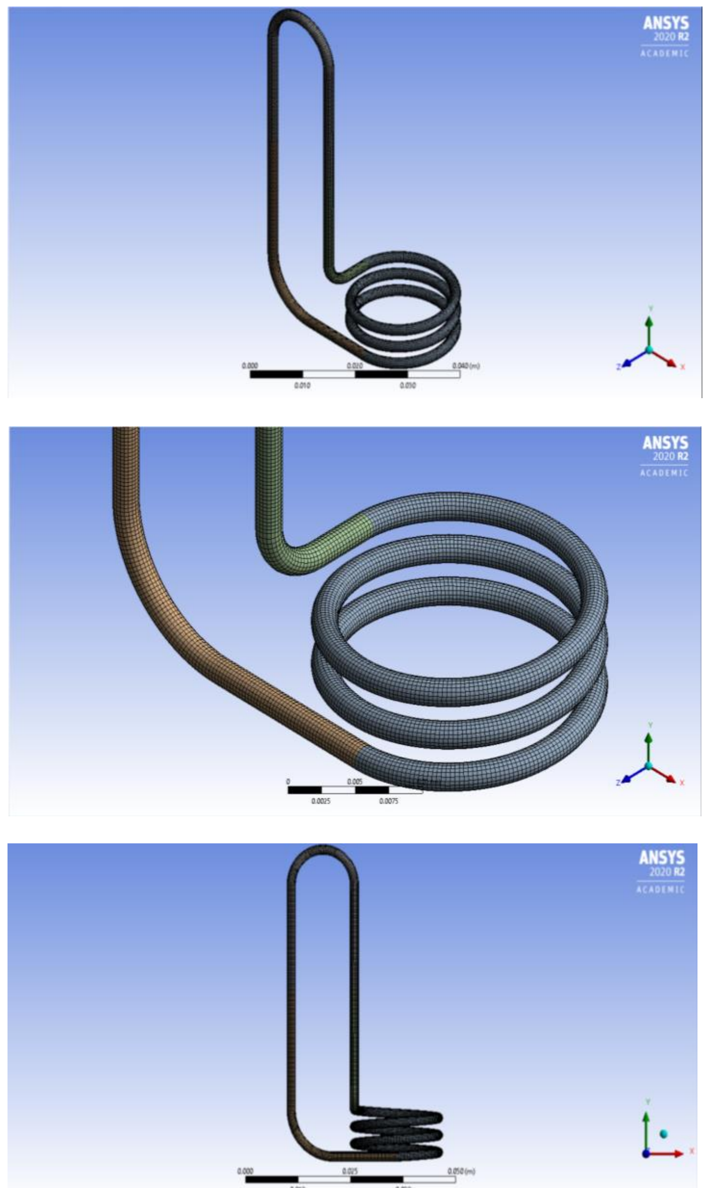

Fig. 6 Mesh generation for evaporator coil CLPHP

4 Flow Simulation

4.1 Single Turn Flat Closed Loop Pulsating Heat Pipe

Thermal analysis of single turn flat CLPHP is carried out using ANSYS fluent the contours of water volume fraction, wall temperature, contours of mass transfer rate and its behavior is studied at various flow time

4.1.1 Contours of Water Volume fraction

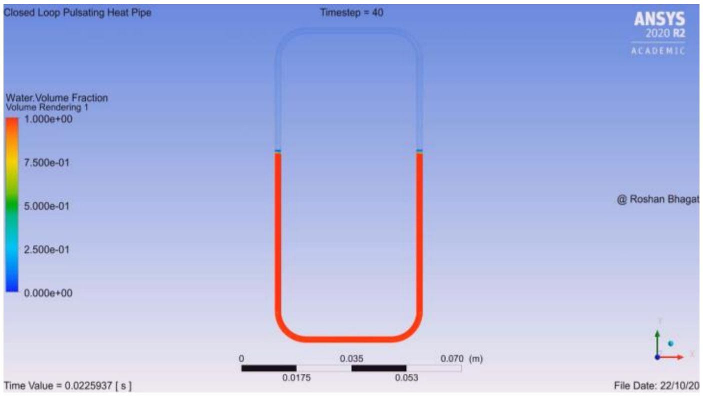

Fig. 7 Contours of water volume fraction at 0 seconds

Fig. 7 shows the contours of water volume fraction where alternative liquid and vapors slug formation are observed at given flow time. Pulsating action drive the fluid towards the condenser section of closed loop pulsating heat pipe.

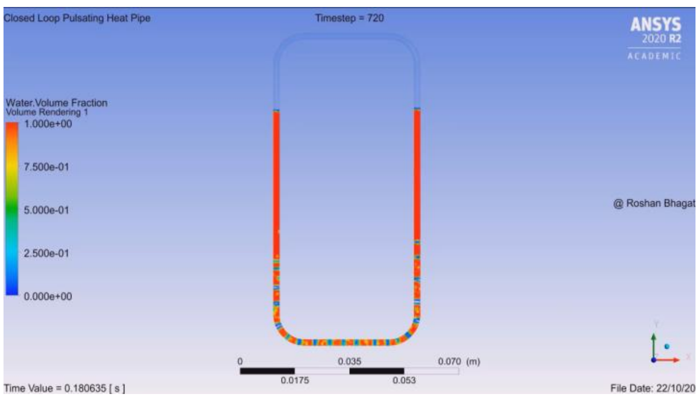

Fig. 8 Contours of water volume fraction at 0.18 Seconds

Fig. 9 shows the fluid flow has been developed and due to condensation, some vapor slug converted to liquid while they reached towards the condenser section. Latent heat as well as sensible heat transfer takes place.

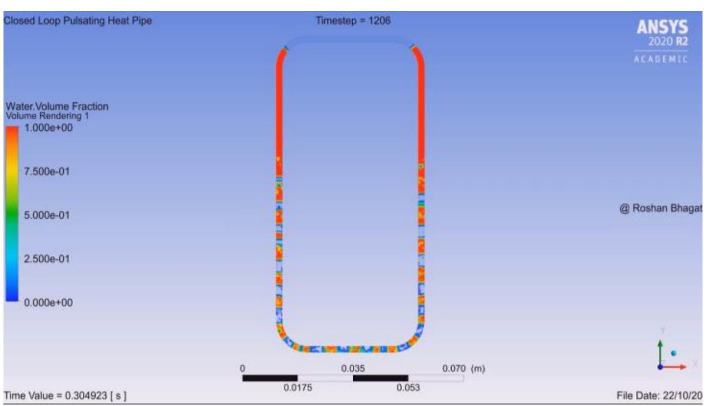

Fig. 9 Contours of water volume fraction at 0.30 Seconds

As the pulsating action takes place difference of pressure and density drives the flow of fluid from evaporator to condenser section. Heat transfer takes place as combination of sensible and latent heat of working fluid.

4.1.2 Contours of Mass Transfer rate

The contours of mass transfer rate help to understand the flow and behavior of fluid during the process of evaporation and condensation.

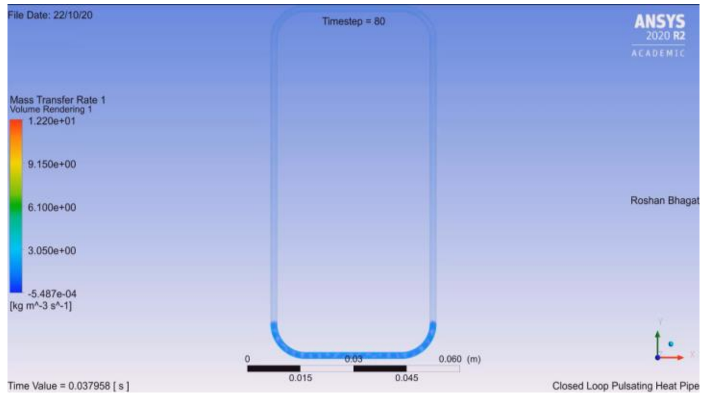

Fig. 10 Contours of Mass transfer Rate at 0 seconds

The contours of mass transfer rate are visualized in the fig. 10 and 11, the mass flow at 0 second and time step of 720 is as shown. The alternating liquid and vapor slug can be easily visualized at given flow time.

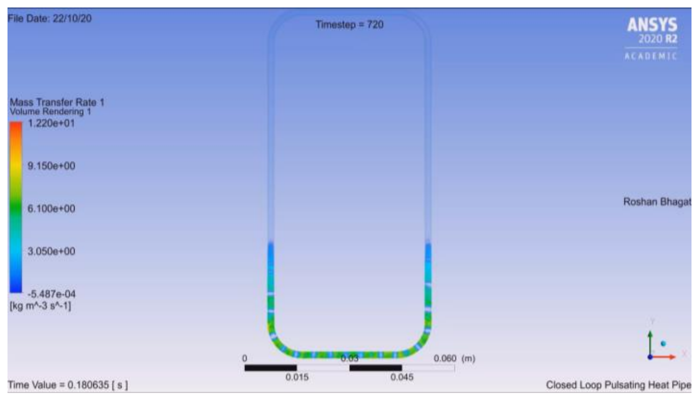

Fig. 11 Contours of mas transfer rate at 0.18 Seconds

The liquid and vapor slugs at time step of 1206 and flow time of 0.30 seconds can be observed, the length of vapor and liquid slug found to be higher in at this flow time. The liquid and vapor slug/plug are travelling towards the condenser.

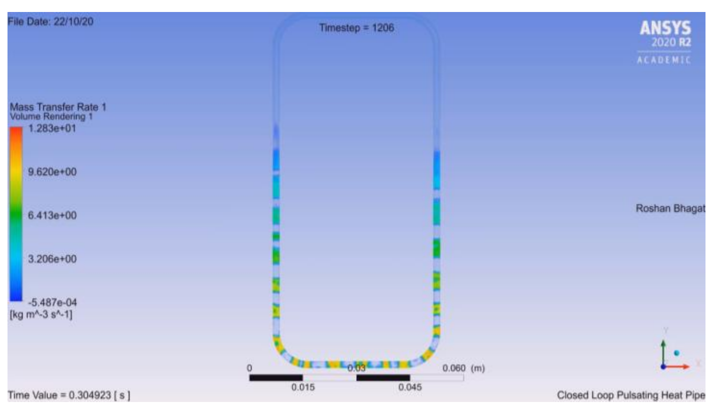

Fig. 12 Contours of mass transfer rate 0.30 seconds

DOI: 10.5098/hmt.16.23
ISSN: 2151-8629

4.1.3 Contours of Wall Temperature

Fig.13 shows the contours of wall temperature to understand the process of evaporation and condensation the temperature at evaporator and condenser will be observed during the flow of fluid. At initial flow time of 0 seconds higher temperature are observed at evaporator.

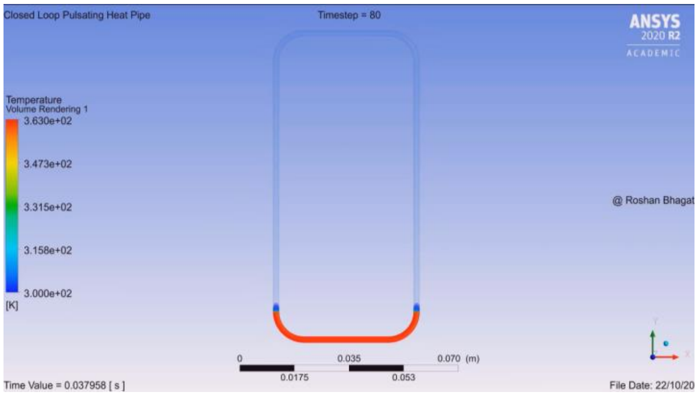

Fig. 13 Contours of wall temperature at 0 seconds

The higher temperature was observed at evaporator section at flow time of 0 seconds whereas as the liquid and vapor slug flow takes place the as heat is carried towards condenser section. The maximum temperature is observed at evaporator section at flow time of 0 seconds.

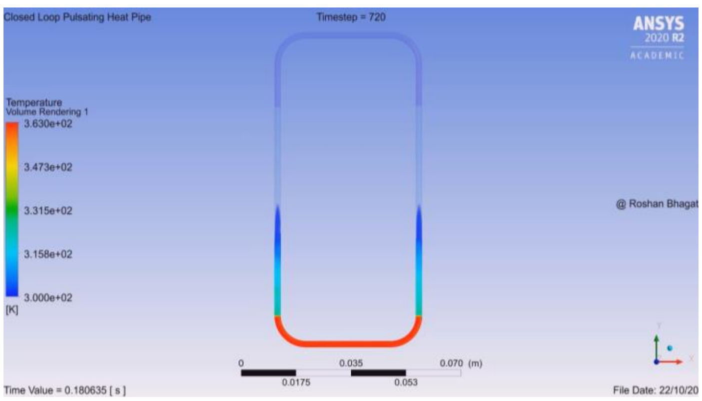

Fig. 14 Contours of wall temperature at 0.18 seconds

The heat absorbed by working fluid in the evaporator section of closed loop pulsating heat pipe is now rejected in the condenser section. The sensible and latent heat are responsible for heat transfer. The contour of wall temperature is studied at various flow time from 0 to 30 seconds. Zone with lower and higher temperature can be observed from contours.

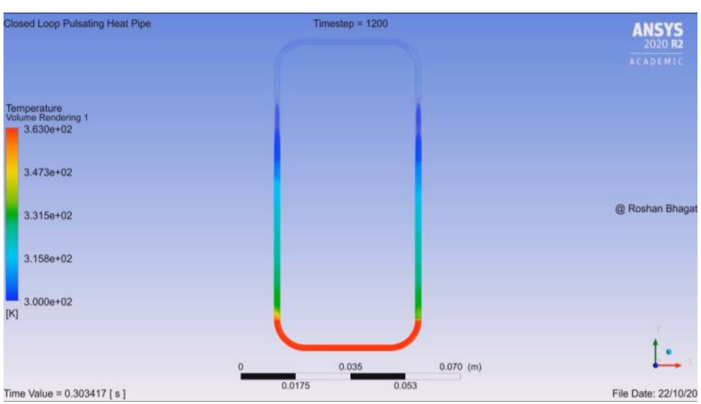

Fig. 15 Contours of wall temperature at 0.30 seconds

4.2 Single Turn Closed Loop Pulsating Heat Pipe

The analysis of single turn closed loop pulsating heat pipe is carried out as shown in the fig. 16 to 19. Contours of water volume fraction. Wall temperature are visualized at various flow time.

4.2.1 Contours of Water Volume Fraction

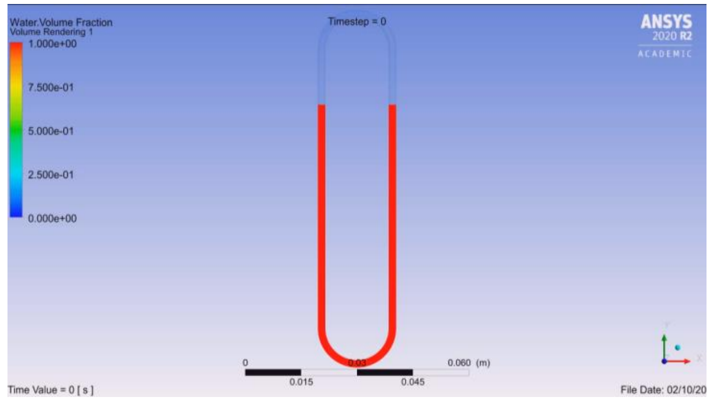

Fig. 16 Contours of water volume fraction at 0 seconds

The alternate liquid and vapor slug formation can be understood with single turn closed loop pulsating heat pipe. Evaporator section has one turn and the condenser section has one turn, combine sensible and latent heat will be responsible for heat transfer.

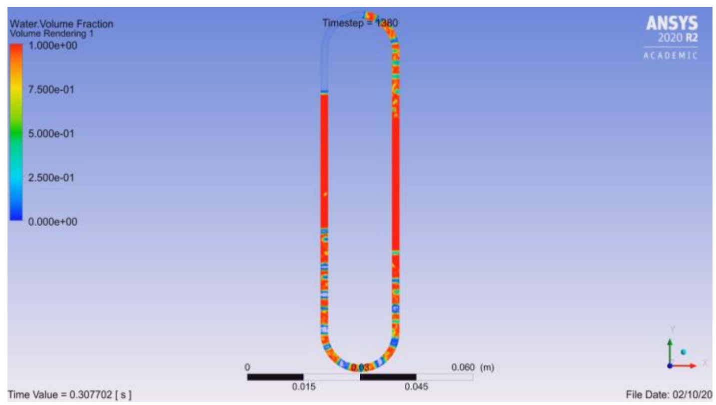

Fig. 17 Contours of water volume fraction at 0.30 Seconds

The flow is found to be fully developed at flow time of 0.58 seconds. The alternative liquid and vapor slugs are clearly visible. The evaporation and condensation phenomenon can be easily understood with the simulation results.

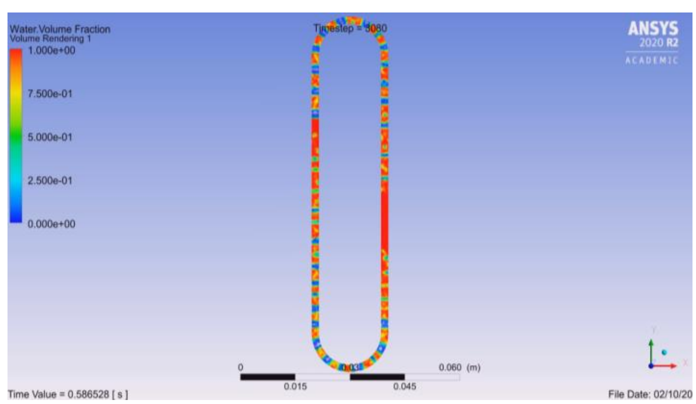

Fig. 18 Contours of water volume fraction at 0.58 seconds

The vapor slug while passing towards the condenser section rejects heat and thus converted in liquid. The flow obtained during the simulation can be different for different experimental run.

DOI: 10.5098/hmt.16.23 ISSN: 2151-8629

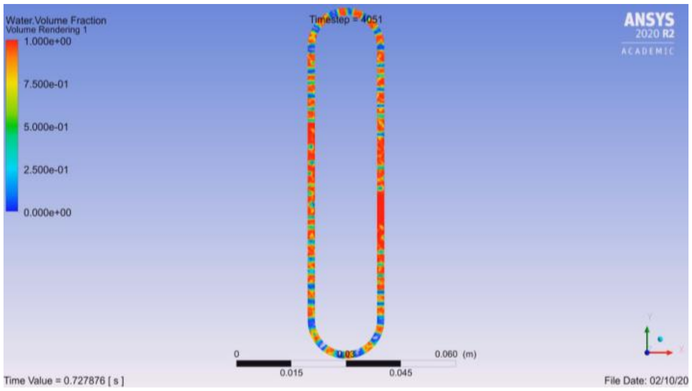

Fig. 19 Contours of water volume fraction at 0.72 seconds

4.2.2 Contours of Wall Temperature

The contours of wall temperature are studied at different flow time. At initial flow time of 0 seconds higher temperatures are observed in the evaporator section of closed loop pulsating heat pipe. The temperature reduction is observed when these liquid and vapor slugs enter the condenser section.

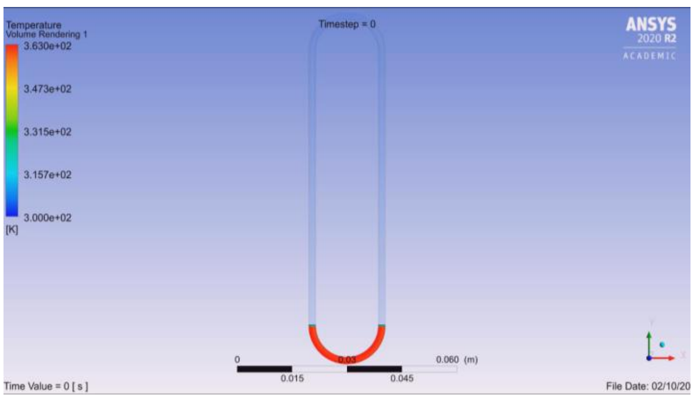

Fig. 20 Contours of wall temperature at 0 Seconds

Various flow times are useful to understand the temperature variation fluid is subjected during the flow from evaporator to condenser section of single turn closed loop pulsating heat pipe.

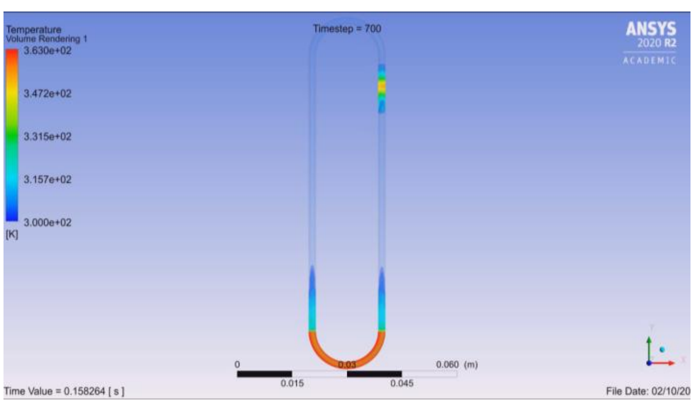

Fig. 21 Contours of wall temperature at 0.15 seconds

Drop in fluid temperature due to rejection of heat are observed at flow time of 0.32 seconds. The heat absorbed by working fluid in the evaporator section is rejected to the secondary fluid present in the condenser section. The condenser tank contains water as secondary fluid where the heat is absorbed.

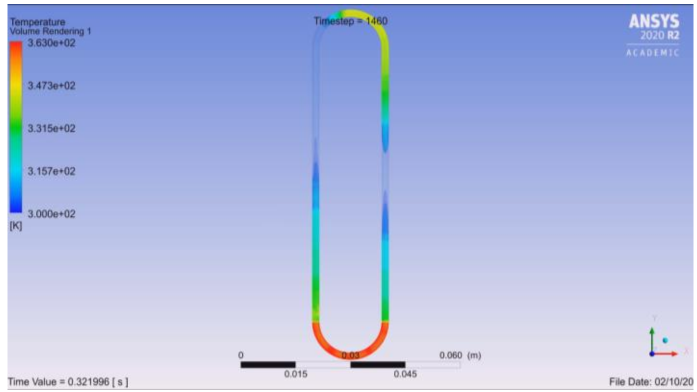

Fig. 22 Contours of wall temperature at 0.32 seconds

The contours of wall temperature are studied at various flow time starting from 0 seconds to 0.72 seconds. The temperature distribution can be more specific while observing the simulation results. Maximum temperature is observed at the evaporator section of heat pipe and minimum temperature is observed at condenser section. As heat transfer occurs heat absorption and rejection take place at evaporator and condenser section of Single Turn Pulsating Heat Pipe.

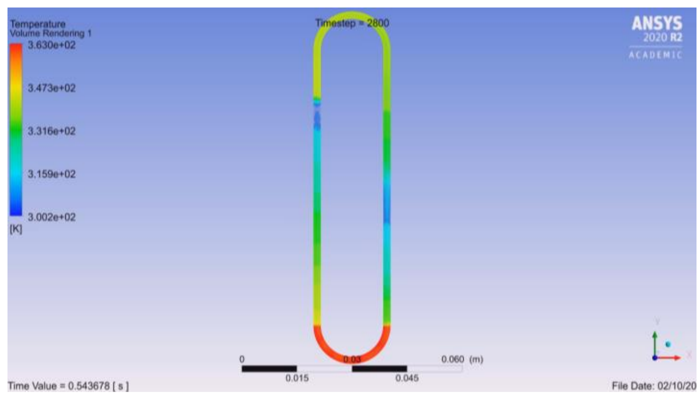

Fig. 23 Contours of wall temperature at 0.54 seconds

The reduction in the temperature can be easily identified at flow time of 0.72 seconds. The evaporator temperature remains high through the process.

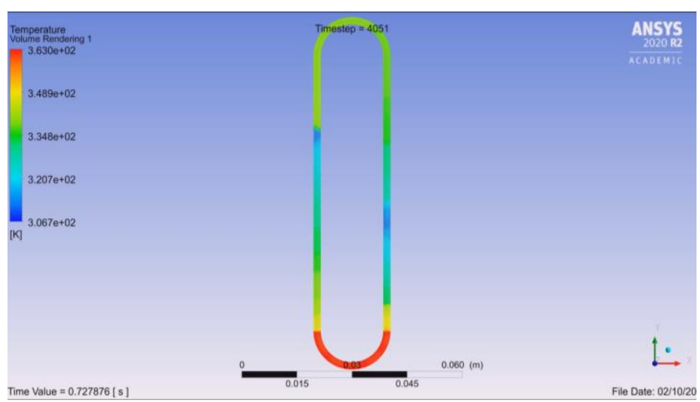

Fig. 24 Contours of wall temperature at 0.72 seconds

4.3 Two Turn Closed Loop Pulsating Heat Pipe

The fluid flow in multiple turn CLPHP is observed in fig. 24 to 29.

4.3.1 Contours of Water Volume Fraction

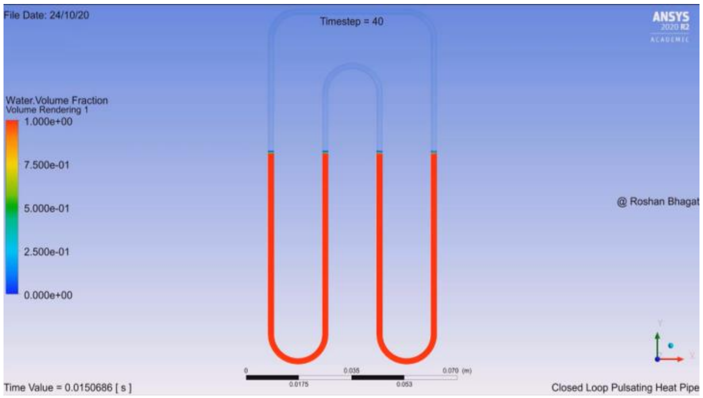

Fig. 25 Contours of water volume fraction at 0 seconds

The contours of water volume fraction at flow time of 0 seconds shows that the steam formation not started during the initial stage of heating. At start of heating the small bubble get condensed at evaporator section before reaching to the other end.

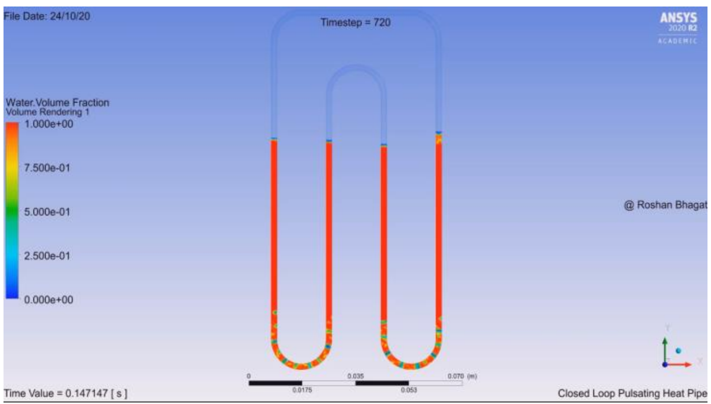

Fig. 26 Contours of water volume fraction at 0.14 seconds

The liquid and vapor slug formation started from the flow time of 0.14 seconds. It is found to be more developed when reached to the flow time of 0.49 seconds. Contours of water volume fraction can be visualized at various flow time that is helpful to understand the behavior of water as working fluid when two turns are present in evaporator section.

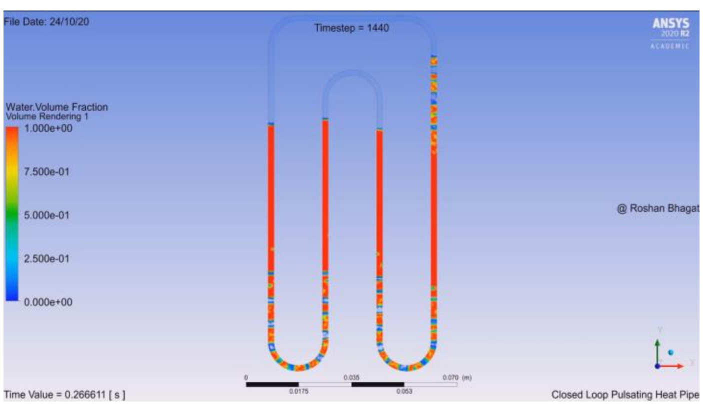

Fig. 27 Contours of water volume fraction at 0.26 seconds

While the vapor slug moves towards the condenser section it was observed that it gets disappear at initial stage of condensation process, these vapor and liquid slug carries heat in the form of sensible and latent heat towards the condenser section.

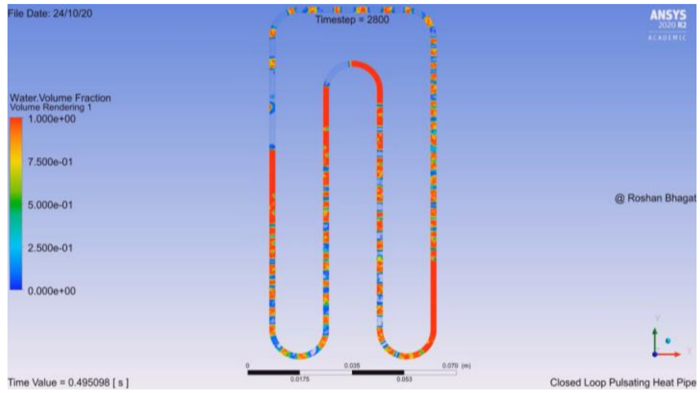

Fig. 28 Contours of volume fraction at 0.49 Seconds

Pulsating action is significant at flow time of 0.58 seconds and time step of 3400. The alternate liquid and vapor slug transport is observed during the flow of fluid, transferring heat from evaporator to condenser section. The fluid flow occurs due to the difference of density between the evaporator and condenser section.

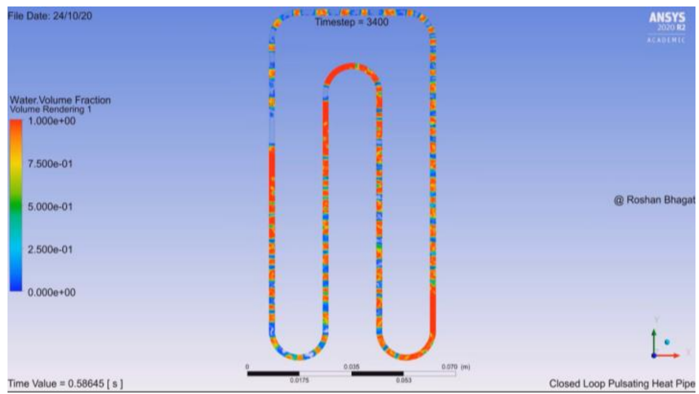

Fig. 29 Contours of volume fraction at 0.58 seconds

4.3.2 Contours of Mass Transfer Rate

The contours of mass transfer rate are studied at various flow times of 0 second to 0.80 seconds. This analysis gives the mass transfer rate of liquid and vapor slug while they move over the entire length of tube.

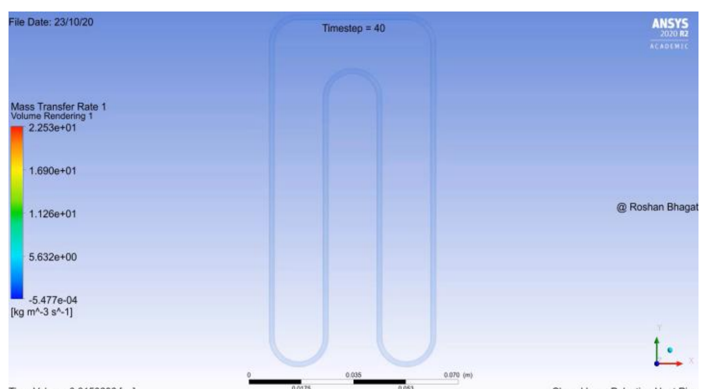

Fig. 30 Contours of mass transfer rate at 0 Seconds

The development of fluid flow is significant after the flow time of 0.31 seconds. Negligible mass flow observed at flow time of 0 seconds. The mass flow rate depends on the heating done at the evaporator section of pulsating heat pipe.

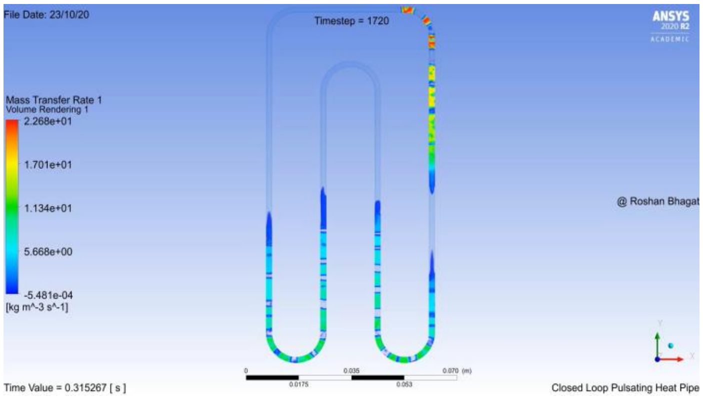

Fig. 31 Contours of mass transfer rate at 0.31

Alternate liquid and vapor slug flow can be observed with contours of mass transfer rate as shown in the fig. 31 of two turn closed loop pulsating heat pipe. The simulation of fluid flow shows flow pattern that developed in a two-turn closed loop pulsating heat pipe at a flow time of 0.49 seconds. The contours of mass transfer rate are observed at different time step and flow time.

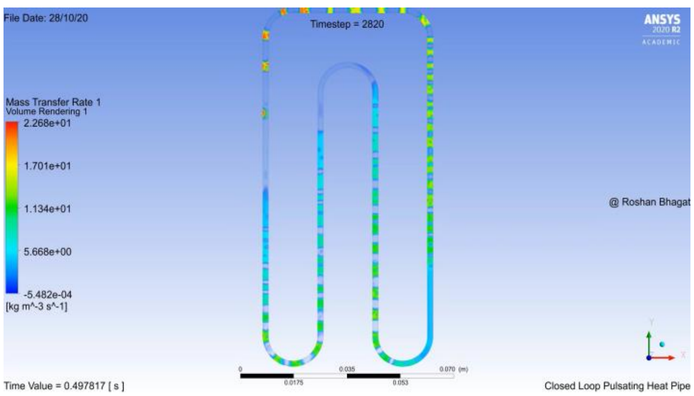

Fig. 32 Contours of mass transfer rate at 0.49 seconds

The alternative liquid and vapor slugs carry heat from evaporator section to the condenser section. The contours of mass flow rate give the mass flow rate at any point in along the length of two turn CLPHP.

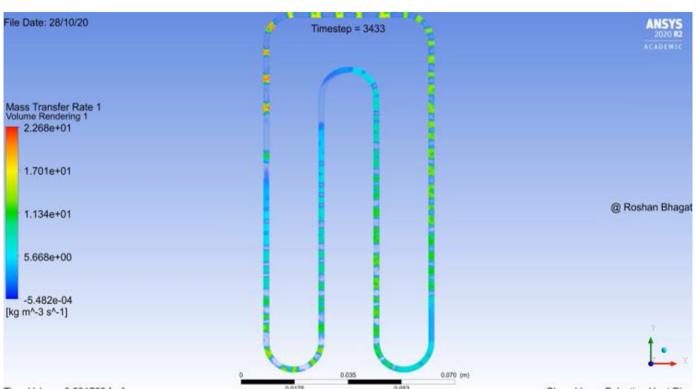

Fig. 33 Contour of mass transfer rate at 0.59 seconds

The contours of mass transfer rate at a flow time of 0.80 seconds shows the fully developed flow pattern of alternate liquid and vapor slug transport from evaporator to the condenser section of Closed Loop Pulsating Heat pipe

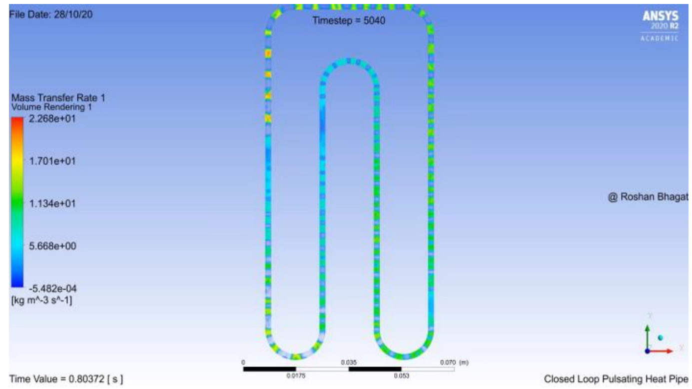

Fig. 34 Contours of mass transfer rate at 0.80 seconds

4.4 Three Turn Closed Loop Pulsating Heat Pipe

Behavior of closed loop pulsating heat pipe with three small turn in evaporator section, two small and one large turn in condenser section is studied from the fig.35 To 46, at different flow time and time step.

4.4.1 Contours of Water Volume Fraction

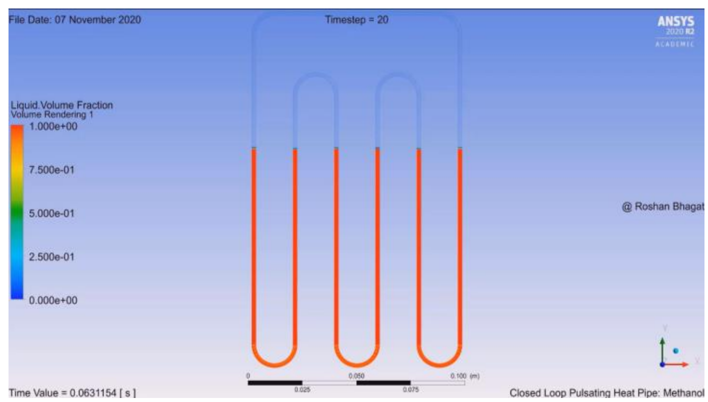

Fig. 35 Contours of volume fraction at 0 Seconds

The development of liquid and vapor slug is observed at flow time of 0.47 seconds. The phenomenon of evaporation and condensation can be best visualized in simulation result.

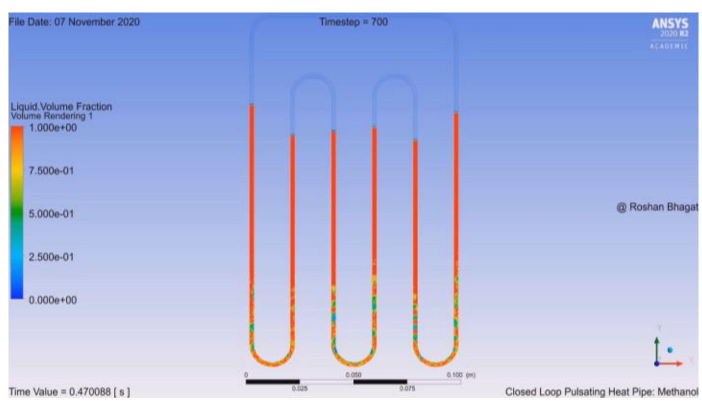

Fig. 36 Contours of volume fraction at time of 0.47 Seconds

The flow pattern i.e. direction of fluid flow is found to be different at each simulation run. The flow pattern depends on the density difference between the evaporator and condenser section.

 Global Digital Central
DOI: 10.5098/hmt.16.23
ISSN: 2151-8629

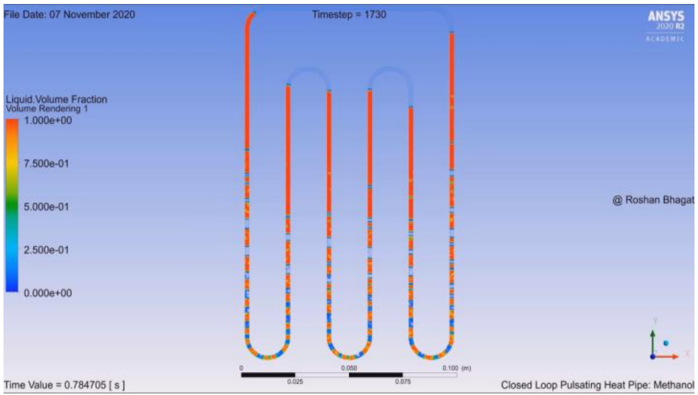

Fig. 37 Contours of volume fraction at flow time of 0.78 Seconds

Initially larger length of liquid and vapor slugs are observed at flow time of 1.11 seconds. The flow visualization helpful in understanding the phenomenon of evaporation and condensation in three turn closed loop pulsating heat pipe.

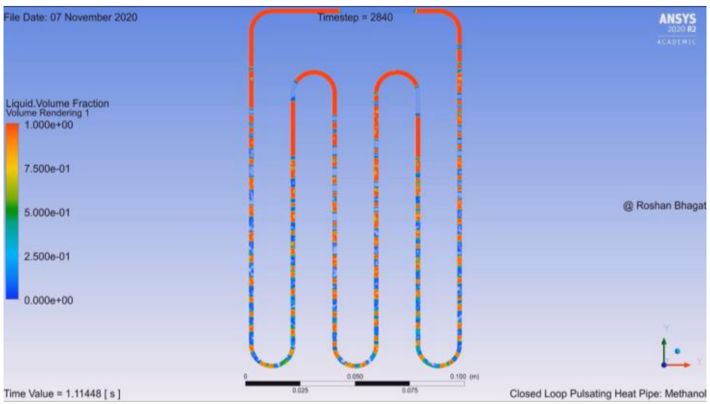

Fig. 38 Contours of volume fraction at flow time of 1.11 Seconds

4.4.1 Contours of Mass Transfer Rate

The mass flow rate is visualized at different flow time as shown below.

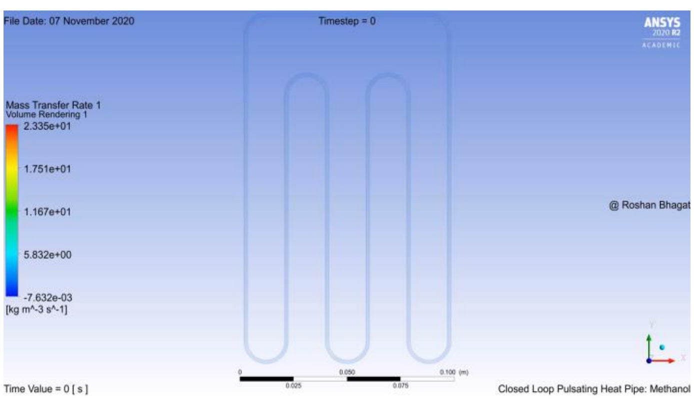

Fig. 39 Contours of mass transfer rate at 0 seconds

At 0 seconds flow is not developed as observed in the fig. 39. The contours of mass transfer rate show the development of fluid flow over the entire length of the tube.

The contours of mass transfer rate show the fluid flow development occurs in the form of alternate liquid and vapor slug. As the flow time increases the mass transfer rate increases.

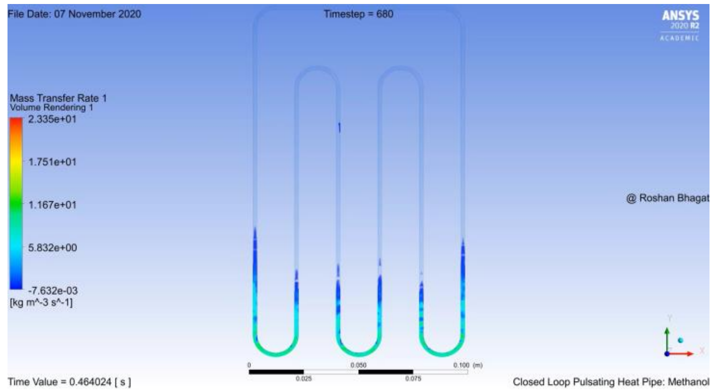

Fig. 40 Contours of mass transfer rate at 0.46 Seconds

At the flow time of 0.46 seconds the flow is developed near to the evaporator section only. The flow pattern is in the form of alternate liquid and vapor slug. The flow development is found significant at flow time of 0.78 seconds at time step of 1720.

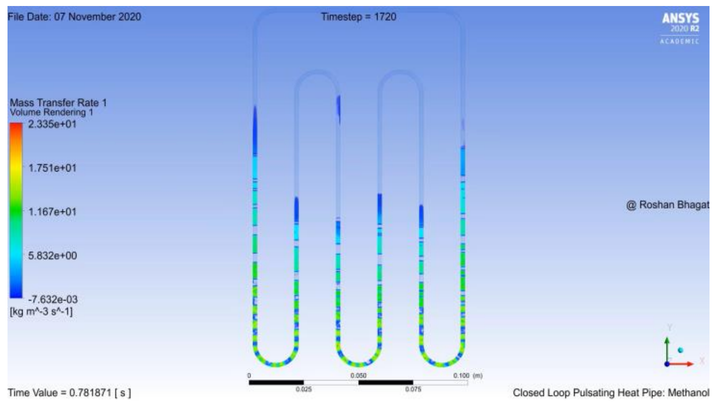

Fig. 41 Contours of transfer rate at 0.78 seconds

The mass flow pattern of liquid in vapor slug enters the region of condenser section where, sensible and latent heat transfer takes place. The flow is said to be fully developed at 1.11 seconds

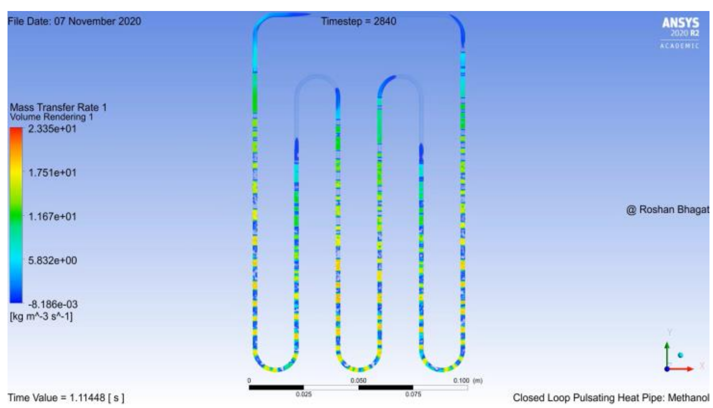

Fig. 42 Contours of mass transfer rate at 1.11 seconds

4.4.3 Contours of Wall Temperature

The contours of wall temperature are important to get the temperature at evaporator and condenser section. At given flow time of 0 seconds. Maximum temperature is observed at evaporator only.

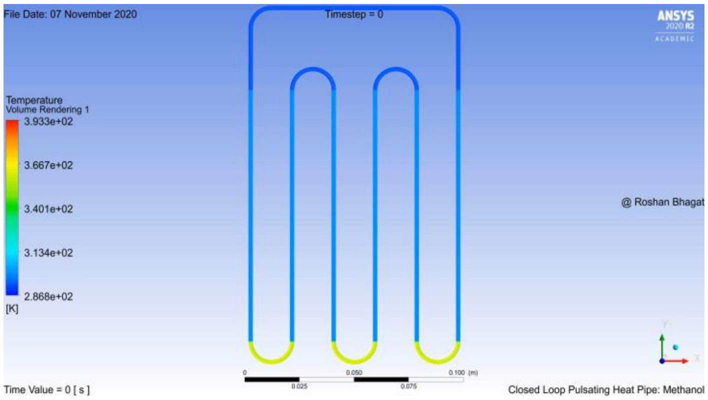

Fig. 43 Contours of wall temperature at 0 seconds

At given time step of 0 heated zones are observed at evaporator section only. At flow time of 0.47 seconds the temperature starts increasing, the color contours can be visualize as shown in Fig. 44. The evaporator section observed to at higher temperature than the condenser section. Heat is first transfer from water bath to the copper tube by convection which subsequently transfer to the working fluid present inside by the conduction heat transfer.

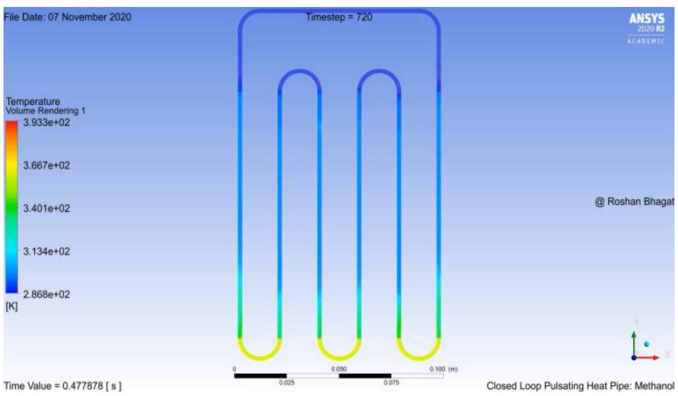

Fig. 44 Contours of wall temperature at 0.47 seconds

As the flow time is increase the temperature enhancement is seen along the length of tube.

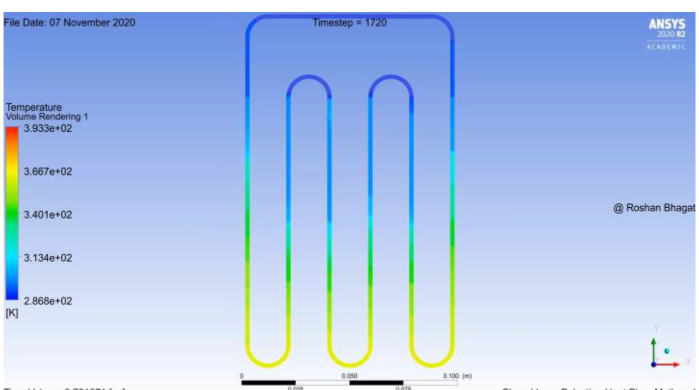

Fig. 45 Contours of wall temperature at 0.78 seconds

The temperature near to the condenser is increased as shown in the Fig. 45. The heat is carried by working fluid in the form of sensible and latent heat towards the condenser section

The contours of wall temperature at the evaporator section are found to be higher at flow time of 1.11 seconds, the temperature increased is also observed near to condenser section. The minimum value of temperature is observed exactly in the condenser it indicates the heat is rejected by working fluid.

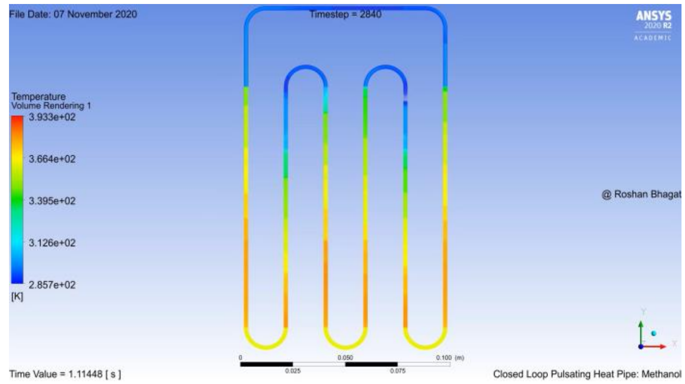

Fig. 46 Contours of wall temperature at 1.11 seconds

4.5 Six Turn Closed Loop Pulsating Heat Pipe

The flow visualization can be observed from fig. 47 to 58 having six small turns in condenser section, one large turn in condenser section and five small turns in condenser section. The contours of water volume fraction, wall temperature and mass flow rates are studied.

4.5.1 Contours of Wall Temperature

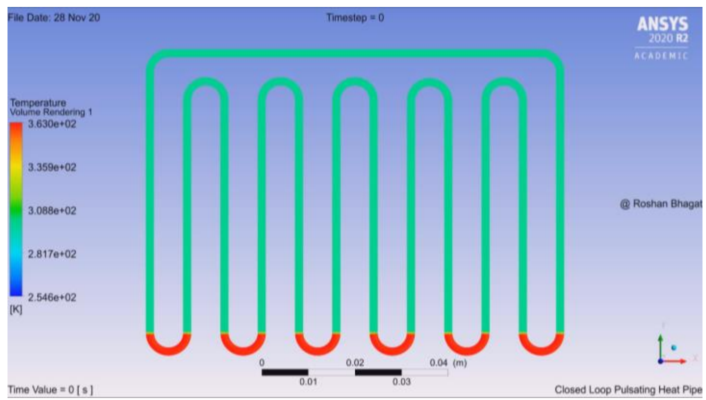

Fig. 47 Contours of wall Temperature at flow time of 0 second

The contours of wall temperature show the temperature started increasing with the application of heat in evaporator section

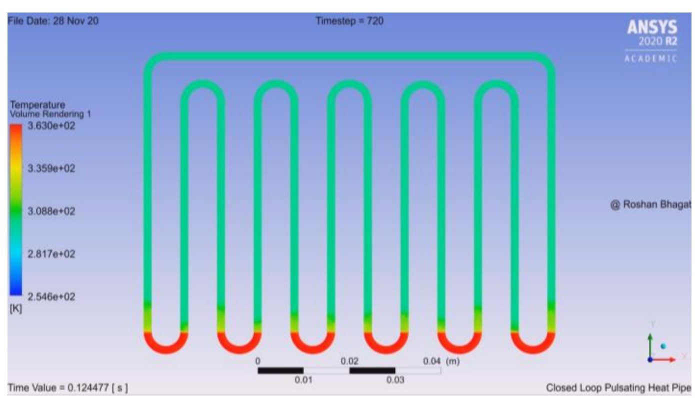

Fig. 48 Contours of wall temperature at flow time of 0.12 second

The wall temperature started to increase as per the observation from the flow time of 0 seconds to 0.27 Seconds. The flow is getting developed and, in the simulation, higher temperature zones are visible in contours of the evaporator section of heat pipe and lower temperature contours are visible in condenser section of heat pipe. Red zones indicate the higher temperature values.

DOI: 10.5098/hmt.16.23

ISSN: 2151-8629

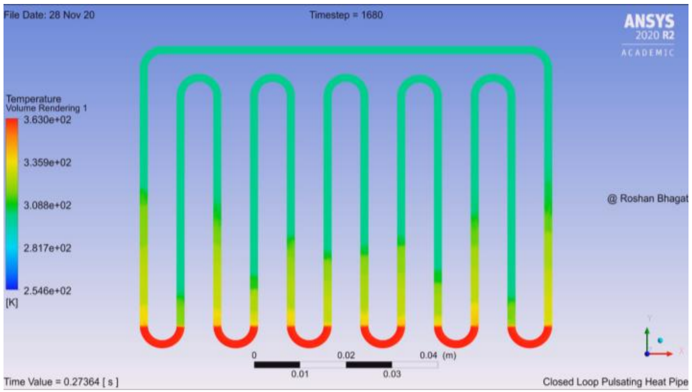

Fig. 49 Contours of wall temperature at flow time 0f of 0.27 second

The higher wall temperature is observed in the contour is the result of sensible and latent heat transfer that takes place when fluid moves from evaporator to the condenser section of CLPHP.

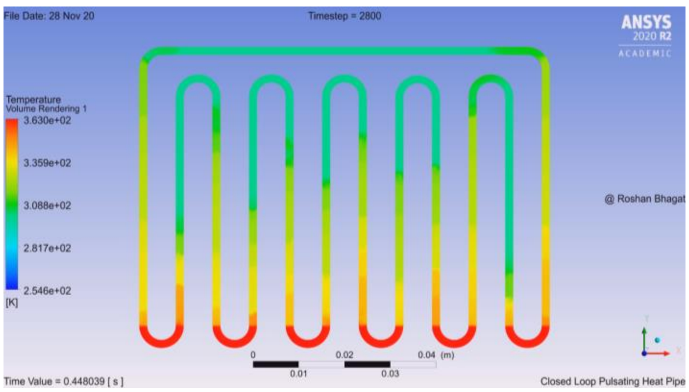

Fig. 50 Contours of wall temperature at flow time of 0.44 seconds

4.5.2 Contours of Water Volume Fraction

The fig. 51 shows the contours of water volume fraction at flow time of 0 seconds. As per the visualization the heating has started and the flow is yet to get developed.

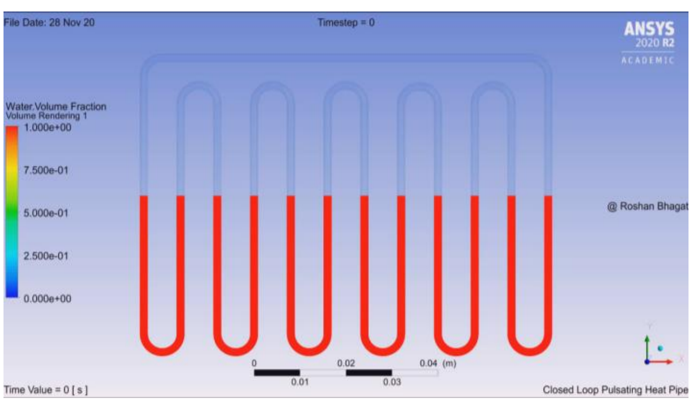

Fig. 51 Contours of volume fraction water at 0 second

The various flow times from Fig. 51 to Fig. 54 shows the development of fluid flow that occurs when the heating is done in the evaporator section. As the diameter is small i.e., critical diameter, alternate liquid and vapor slug formations are observed throughout the simulation. The phenomenon of condensations also observed during the development of flow of fluid.

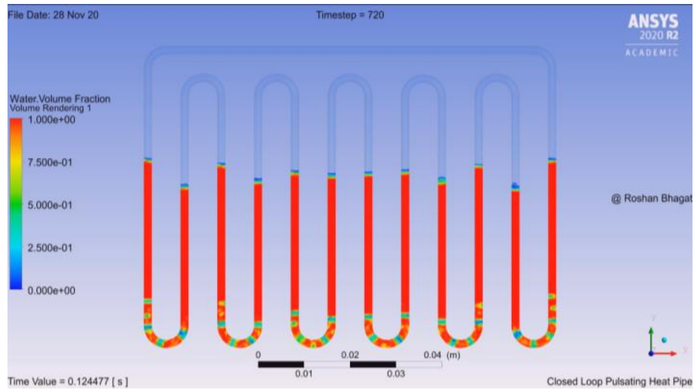

Fig. 52 Contours of volume fraction at flow time of 0.12 second

The below Fig. shows the development of fluid flow. The alternate liquid vapor slug formation and bubble transport are observed in simulation.

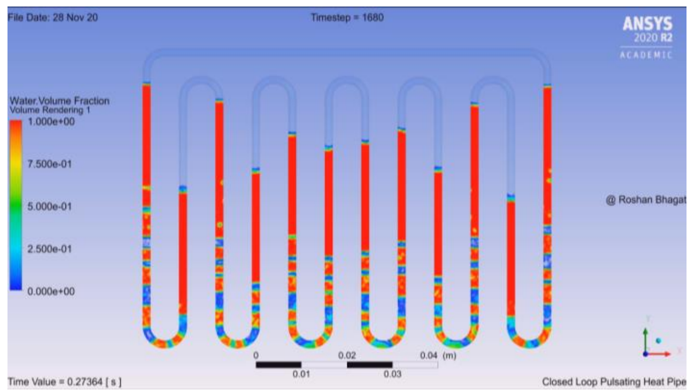

Fig. 53 Contours of volume fraction of water at 0.27 Seconds

At the flow time of 0.44 seconds the complex phenomenon of evaporation and condensation are visualized. The vapor slug transformed into liquid is observed as vapor travel to condenser section. The flow of fluid is due to the density difference between evaporator and condenser section of CLPHP.

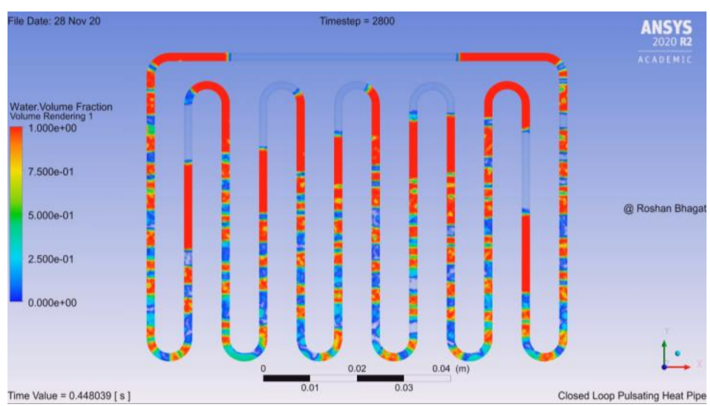

Fig. 54 Contours of volume fraction of water at 0.44 seconds

4.5.3 Contours of Mass Transfer Rate

The contours of mass transfer rate for water shows the mixture of water and steam the phase transformation during the process of heating. Better visualization is observed from the flow time of 0 seconds to the flow time of 0.44 seconds. Negligible mass transfer rate is observed at flow time of 0 seconds, however the same is developed as shown in Fig. 55 to 58.

DOI: 10.5098/hmt.16.23

ISSN: 2151-8629

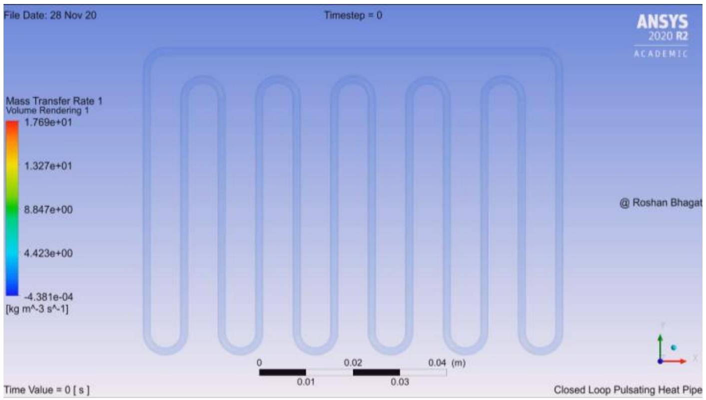

Fig. 55 Contours of mass flow rate at 0 second

The contours of mass transfer rate can be visualized on the left-hand side of the fig. 55. At the start of heating process the mass transfer rate found to be negligible flow development is observed at given time step of 0. The fluid flow development occurs due to density difference of fluid between the evaporator and condenser section. The self-sustain motions can different in different direction for different trial run.

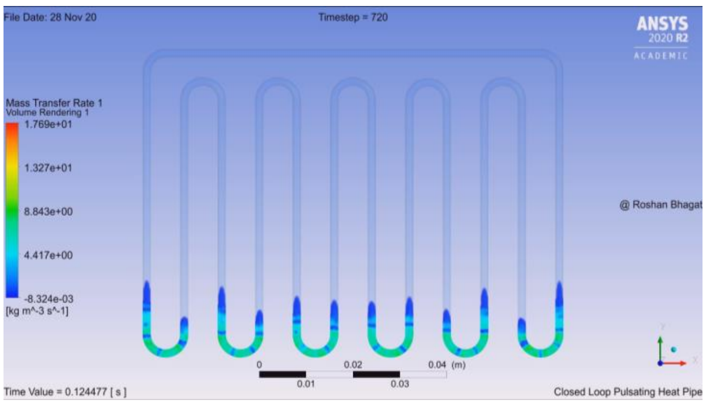

Fig. 56 Contours of mass flow rate at 0.12 seconds

At the flow time of 0.12 seconds the flow development is observed. With smaller mass transfer rate, the flow development is observed near to the evaporator section of heat pipe only.

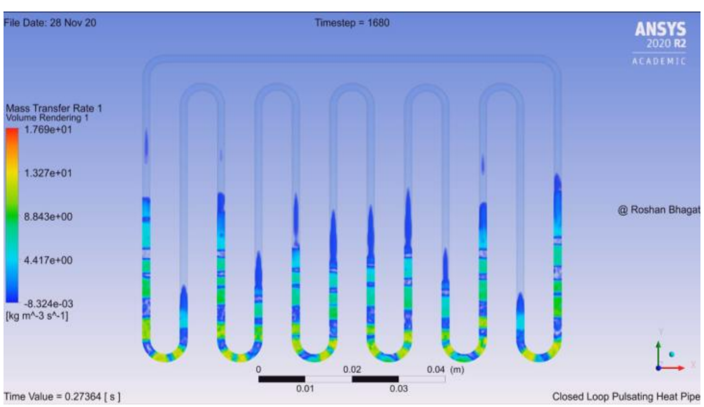

Fig. 57 Contours of mass flow rate at 0.27 Seconds

As the flow time increases the liquid and vapor enhancement is seen. The liquid vapor bubbles reach to condenser section for rejection of heat. The mass transfer rate is found to be higher in the evaporator section of heat pipe. Red zones indicate the higher mass transfer rate at given flow time of 0.44 seconds. Alternate liquid and vapor slug are responsible for heat transfer.

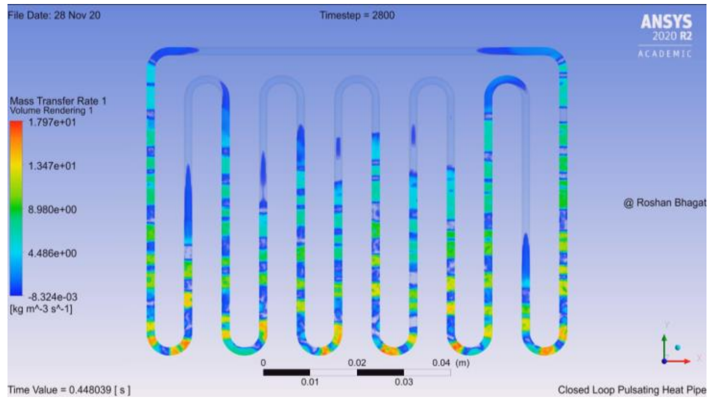

Fig. 58 Contours of mass flow rate at 0.44 seconds

4.6 Evaporator Coil Closed Loop Pulsating Heat Pipe

Closed loop pulsating heat pipe with coil turns in evaporator section is studied, with contours of water volume fraction, contours of wall temperature. The flow behavior is observed at various flow time.

4.6.1 Contours of Water Volume Fraction

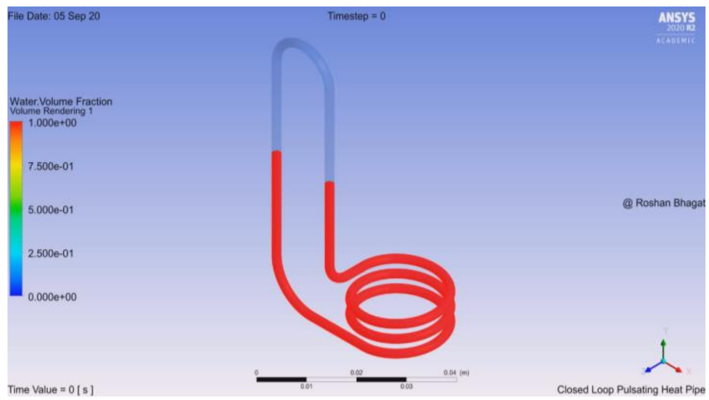

Fig. 59 Contours of water volume fraction at 0 Seconds

The Fig. 60 shows that the heating has started in the evaporator section small vapor bubbles can also be visualized from the flow development. The red zone indicates the presence of water.

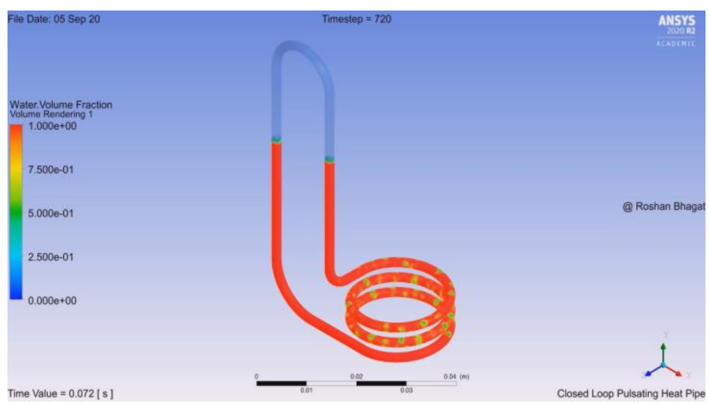

Fig. 60 Contours of water volume fraction 0.07 Seconds

The liquid and vapor slug flow can be observed at given flow time of 0.14 seconds. The liquid and vapor slug movement are observed from evaporator to condenser section. During the initial stage the vapor gets condensed as soon as it enters the condenser section of evaporator coil closed loop pulsating heat pipe.

Global Digital Central
ISSN: 2151-8629

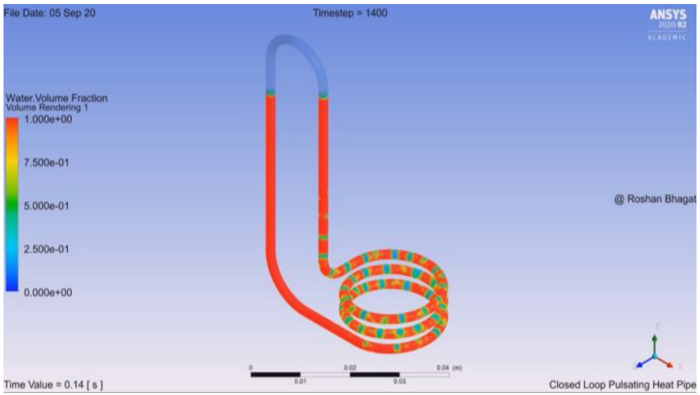

Fig. 61 Contours of water volume fraction at 0.14 Seconds

The liquid and vapors slug development are rapid at the flow time of 0.28 seconds. The visualization shows the alternate liquid and vapor bubble transport phenomenon starting from evaporator section to the condenser section. The vapor slug found to get condense during the entry region where vapor gets converted into liquid.

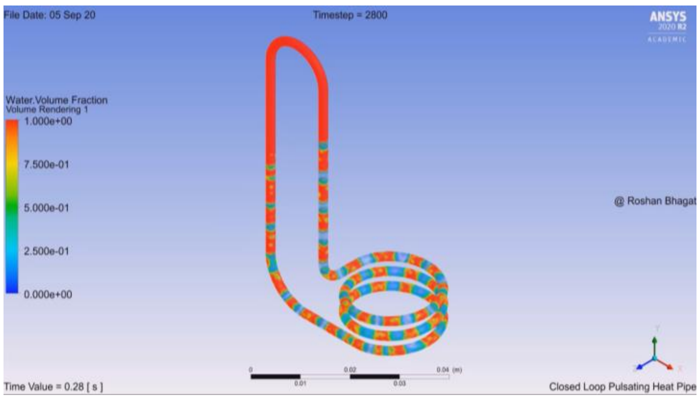

Fig. 62 Contours of water volume fraction at 0.28 Seconds

The length of vapor and liquid slug formed found to be more at flow time of 0.50 seconds. The direction of fluid flow circulation depends on the difference in densities of working fluid used. The flow pattern may be different for different experimental run.

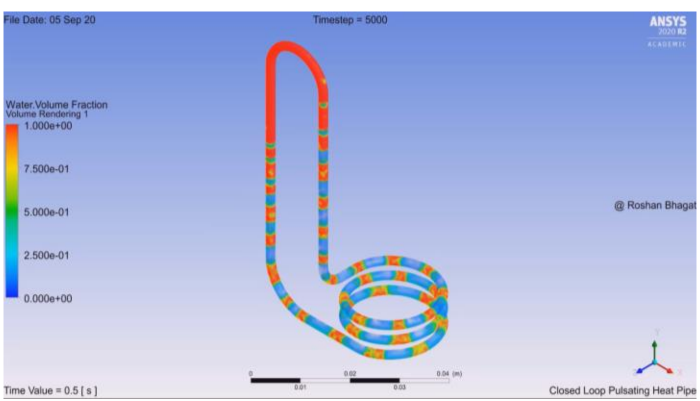

Fig. 63 Contours of water volume fraction at 0.50 seconds

4.6.2 Contours of Wall Temperature

The wall temperature is visualized at different flow time as shown in fig. 64 to 66 starting from 0 seconds to 0.5 seconds. Red zones are observed at evaporator section of heat pipe.

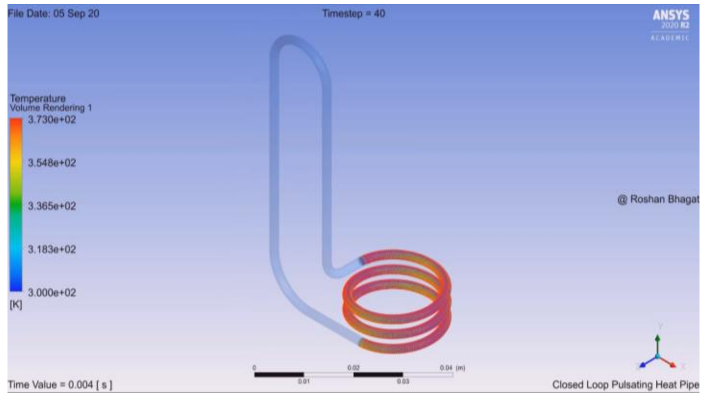

Fig. 64 Contours of wall temperature at 0 seconds

The alternate liquid and vapor slug transport take the heat from evaporator to the condenser section. Contours of wall temperature helps in understanding the evaporation and condensation process in evaporator coil closed loop pulsating heat pipe. The difference of density is responsible for fluid flow from evaporator to the condenser section

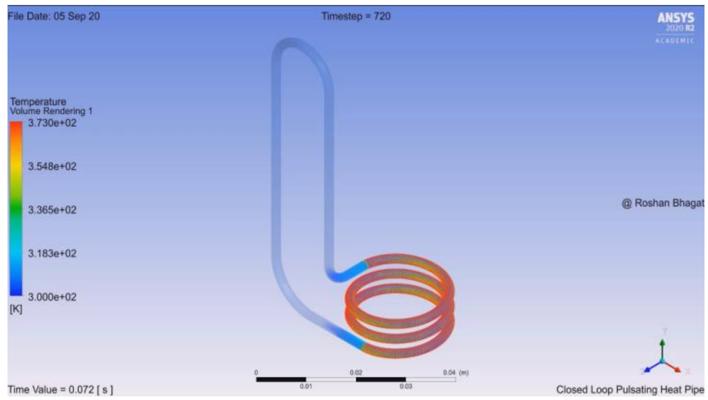

Fig. 65 Contours of wall temperature at 0.072 seconds

The increase in wall temperatures is observed at given flow time of 0.14 seconds. The variation in the color contours can be observed as the heating in done in the evaporator section. The gradual temperature variation is observed from evaporator to condenser section.

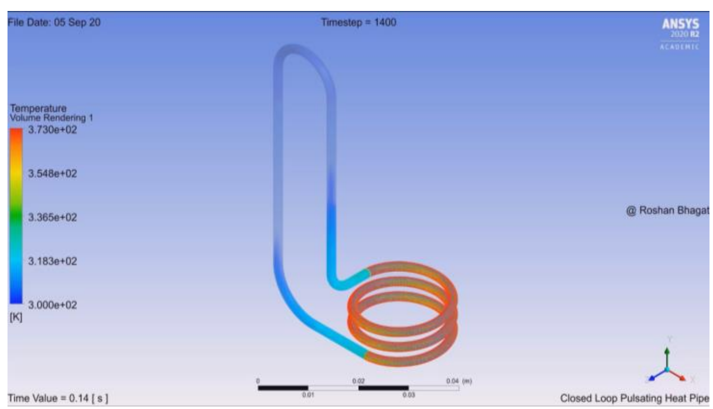

Fig. 66 Contours of wall temperature at 0.14 seconds

The contours of wall temperature show the temperature distribution along the length of the pulsating heat pipe. There is increase in the value of temperature at condenser at flow time of 0.28 seconds. The sensible and latent heat transfer is primary reason for the temperature change at the condenser section.

Frontiers in Heat and Mass Transfer (FHMT), 16, 23 (2021)
DOI: 10.5098/hmt.16.23
Global Digital Central
ISSN: 2151-8629

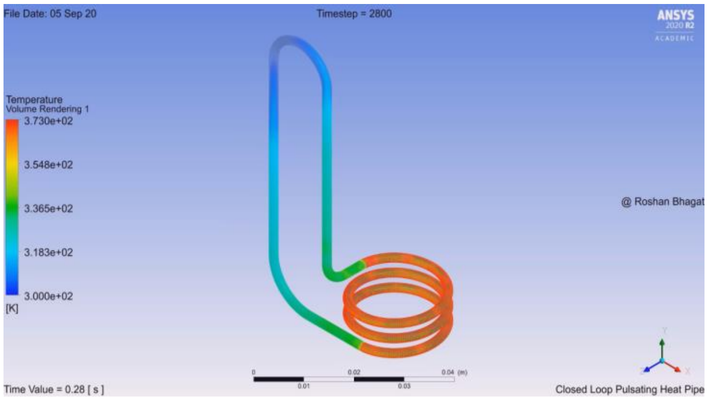

Fig. 67 Contours of wall temperature at 0.28 seconds

The contours of wall temperature show the heat carried by liquid and vapor slug while moving from evaporator to condenser section. The drop in temperature was observed in condenser section. The closed loop pulsating heat pipe with coil in evaporator section looks promising in higher heat transfer.

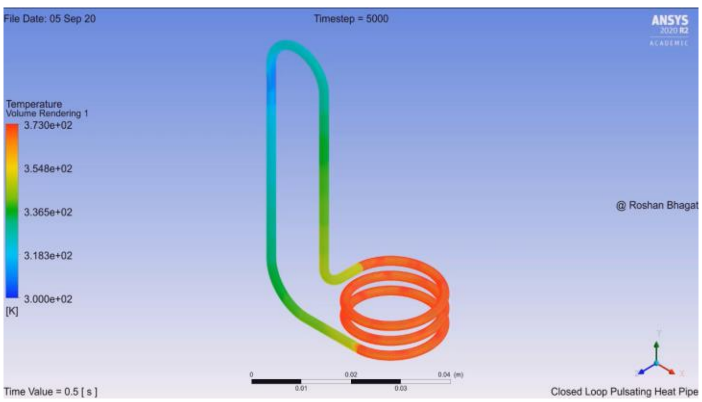

Fig. 68 Contours of wall temperature at 0.5 seconds

5 Conclusion

The Numerical analysis of closed loop pulsating heat pipe is carried out by using different 3D geometries. The flow visualization using CFD tools helped in predicting the flow of fluid, the behavior is studied at various flow time. The contours of liquid volume fraction, contours of wall temperature and contours of mass flow rate are visualized. For few geometries the flow is getting developed at lower flow time while for some other it has developed at higher flow time.

The phenomenon of evaporation and condensation best understood with CFD results thus, this will be helpful in selection of geometry for given closed loop pulsating heat pipe. Also, it is observed that as all the different combination of 3D geometries used has same inner diameter of 2mm the liquid and vapor slug formation take place, if the diameter is more than 2mm these pulsations does not take place. The aspect ratio i.e., length to diameter ratio is also important in order to have the pulsating action so as to transfer heat in the form of sensible and latent heat. Evaporator coils closed loop pulsating heat pipe seems promising for cooling of battery and other electronic components. Best visualization results are obtained with the evaporator coils closed loop pulsating heat pipe.

Nomenclature

CLPHP	Closed Loop Pulsating Heat Pipe
CFD	Computational Fluid Dynamics
CPU	Central Processing Unit
VOF	Volume of Fluid
FR	Filling Ratio
3D	Three Dimensional
PHP	Pulsating Heat Pipe
$\dot{m}$	Mass transfer rate
l	liquid
v	Vapor
t	Time
P	Pressure
T	Temperature
F_{VOL}	Volume Force
µ	Viscosity
P	Pressure
E	Energy

References

Khandekar S., and Groll M., 2003, “On the Definition of Pulsating Heat Pipe,” Proceedings of 5th Minsk International Seminar (Heat Pipes, Heat Pumps and Refrigerators), Minsk, Belarus.

Charoensawan P., Khandekar S., and Groll M., 2004, “Closed Loop and Open Loop Pulsating Heat Pipes,” Proceedings of 13th International Heat Pipe Conference, Shanghai, China, 21-25.

Dadong Wang, and Xiaoyu. Cui, 2010, “Experimental Research on Pulsating Heat Pipe with Different Mixtures Working Fluids,” the 21st International Symposium on Transport Phenomena 2-5 November, Kaohsiung City, Taiwan.

Narasimha K. R., Sridhara S.N., Rajagopal M.S., and Seetharamu K.N., 2012, “Influence of Heat Input, Working Fluid and Evacuation Level on the Performance of Pulsating Heat Pipe,” Journal of Applied Fluid Mechanics, **5**(2), 33-42.

Charoensawan, P., Khandekar, S., Groll, M., and Terdtoon, P., 2003 “Closed Loop Pulsating Heat Pipes- Part A: Parametric Experimental Investigations,” Applied Thermal Engineering, **23**(16), 2009-2020. http://dx.doi.org/10.1016/s1359-4311(03)00159-5.

Bhagat R.D., and Watt K.M., 2015, “Experimentation to Predict the Thermal Performance of Closed Loop Pulsating Heat Pipe with Acetone and Methanol as Working Fluid,” International Journal for Research in Engineering and Technology, **4**(4), 23-27. http://dx.doi.org/10.15623/ijret.2015.0404005 .

Fairley, J.D., Thompson, S.M., and Anderson, D., 2015, “Time–Frequency Analysis of Flat-Plate Oscillating Heat Pipes,” International Journal of Thermal Science, **91**, 113–124. https://doi.org/10.1016/j.ijthermalsci.2015.01.001.

Patel, V.M., and Mehta, H.B., 2017, “Influence of Working Fluids on Startup Mechanism and Thermal Performance of a Closed Loop Pulsating Heat Pipe,” Applied Thermal Engineering, **110**, 1568–1577. https://doi.org/10.1016/j.applthermaleng.2016.09.017.

Akachi H., 1990, “Structure of a Heat Pipe,” U.S. Patent 4921041.

Qu, J., Zhao J.T., and Rao, Z.H., 2017, “Experimental Investigation on the Thermal Performance of Three-Dimensional Oscillating Heat Pipe,” International Journal of Heat Mass Transfer, **109**, 589–600**.** https://doi.org/10.1016/j.ijheatmasstransfer.2017.02.040.

Kearney, D.J., Suleman, O., Griffin, J., and Mavrakis, G., 2016, “Thermal Performance of A PCB Embedded Pulsating Heat Pipe for Power Electronics Applications,” Applied Thermal Engineering, **98**, 798–809. https://doi.org/10.1016/j.applthermaleng.2015.11.123.

Dang, C., Jia, L., and Lu, Q., 2017, “Investigation on Thermal Design of a Rack with The Pulsating Heat Pipe for Cooling CPUs,” Applied Thermal Engineering, **110**, 390–398. https://doi.org/10.1016/j.applthermaleng.2016.08.187.

Maydanik, Y.F., Dmitrin, V.I., and Pastukhov, V.G., 2009, "Compact Cooler for Electronics on the Basis of a Pulsating Heat Pipe," Applied Thermal Engineering, **29**, 3511–3517.
https://doi.org/10.1016/j.applthermaleng.2009.06.005.

Lv, L., Li, J., and Zhou, G., 2017, "A Robust Pulsating Heat Pipe Cooler for Integrated High Power LED Chips," Heat Mass Transfer, **53**, 3305–3313.
https://doi.org/10.1007/s00231-017-2050-3.

Natsume, K., Mito, T., Yanagi, N., Tamura, H., Tamada, T., Shikimachi, K., Hirano, N., and Nagaya, S., 2011, "Heat Transfer Performance of Cryogenic Oscillating Heat Pipes for Effective Cooling of Superconducting Magnets," Cryogenics, **51**, 309–314.
https://doi.org/10.1016/j.cryogenics.2010.07.001.

Arab, M., Soltanieh, M., and Shafii, M.B., 2012, "Experimental Investigation of Extra-Long Pulsating Heat Pipe Application in Solar Water Heaters," Experimental Thermal Fluid Science, **42**, 6–15**.** https://doi.org/10.1016/j.expthermflusci.2012.03.006.

Kargarsharifabad, H., Jahangiri Mamouri, S., Shafii, M.B., and Taeibi Rahni, M., 2013, "Experimental Investigation of The Effect of Using Closed-Loop Pulsating Heat Pipe on The Performance of a Flat Plate Solar Collector," Journal of Renewable Sustainable Energy, **5**. https://doi.org/10.1063/1.4780996.

Khodami, R., Abbas Nejad, A., Ali, M.R., and Khabbaz, 2016, "Experimental Investigation of Energy and Exergy Efficiency of a Pulsating Heat Pipe for Chimney Heat Recovery," Sustainable Energy Technology Assessment, **16**, 11–17.
https://doi.org/10.1016/j.seta.2016.04.002.

Clement, J., and Wang, X., 2013, "Experimental Investigation of Pulsating Heat Pipe Performance with Regard to Fuel Cell Cooling Application," Applied Thermal Engineering, **50**, 268–274. https://doi.org/10.1016/j.applthermaleng.2012.06.017.

Burban, G., Ayel, V., Alexandre, A., Lagonotte, P., Bertin, Y., and Romestant, C., 2013, "Experimental Investigation of a Pulsating Heat Pipe for Hybrid Vehicle Applications," Applied Thermal Engineering, **50**, 94–103.
https://doi.org/10.1016/j.applthermaleng.2012.05.037.

Deng, H.R., Liu, Y.M., Ma, R.F., Han, D.Y., Gan, Z.H., and Pfotenhauer, J.M., 2015, "Experimental Investigation on A Pulsating Heat Pipe with Hydrogen," IOP Conference Series Material Science and Engineering, **101**, 1–8.
https://doi.org/10.1088/1757-899X/101/1/012065.

Nuntaphan, S., Vithayasai, N., Vorayos, N., Vorayos, T., and Kiatsiriroat, 2009, "Use of Oscillating Heat Pipe Technique as Extended Surface in Wire-On-Tube Heat Exchanger for Heat Transfer Enhancement," International Communication in Heat Mass Transfer, **37**(3), 287–292.
https://doi.org/10.1016/j.icheatmasstransfer.2009.11.006.

Tong B.Y., Wong T.N. and Ooi K.T., 2001, "Closed Loop Pulsating Heat Pipe," Applied Thermal Engineering, **21**(18), 1845-1862.
https://doi.org/10.1016/S1359-4311(01)00063-1

Dadong Wang, and Xiaoyu. Cui, 2010, "Experimental Research on Pulsating Heat Pipe with Different Mixtures Working Fluids," The 21^{st} International Symposium on Transport Phenomena, 2-5 November, Kaohsiung City, Taiwan.

Bhagat R.D., and Watt K.M., 2015, "An Experimental Investigation of Heat Transfer Capability and Thermal Performance of Closed Loop Pulsating Heat Pipe with A Hydrocarbon as Working Fluid," Frontiers in Heat Pipes, **6**(7).
http://dx.doi.org10.5098/fhp.6.7

Bhagat R.D., 2016, "An Experimental Investigation of Thermal Performance of Conventional Heat Pipe with Water, Acetone and Methanol as Working Fluid," Frontiers in Heat Pipes, **7**(4), http://dx.doi.org/10.5098/Fhp.7.4